

V25 - Stochastic Dynamics simulations of a photosynthetic vesicle

where bioinformatics meets biophysics

I Introduction: prelude photosynthesis

II Process view and geometric model of a chromatophore vesicle
Tihamér Geyer & V. Helms (Biophys. J. 2006a, 2006b)

III Stochastic dynamics simulations
T. Geyer, Florian Lauck & V. Helms (J. Biotechnol. 2007)

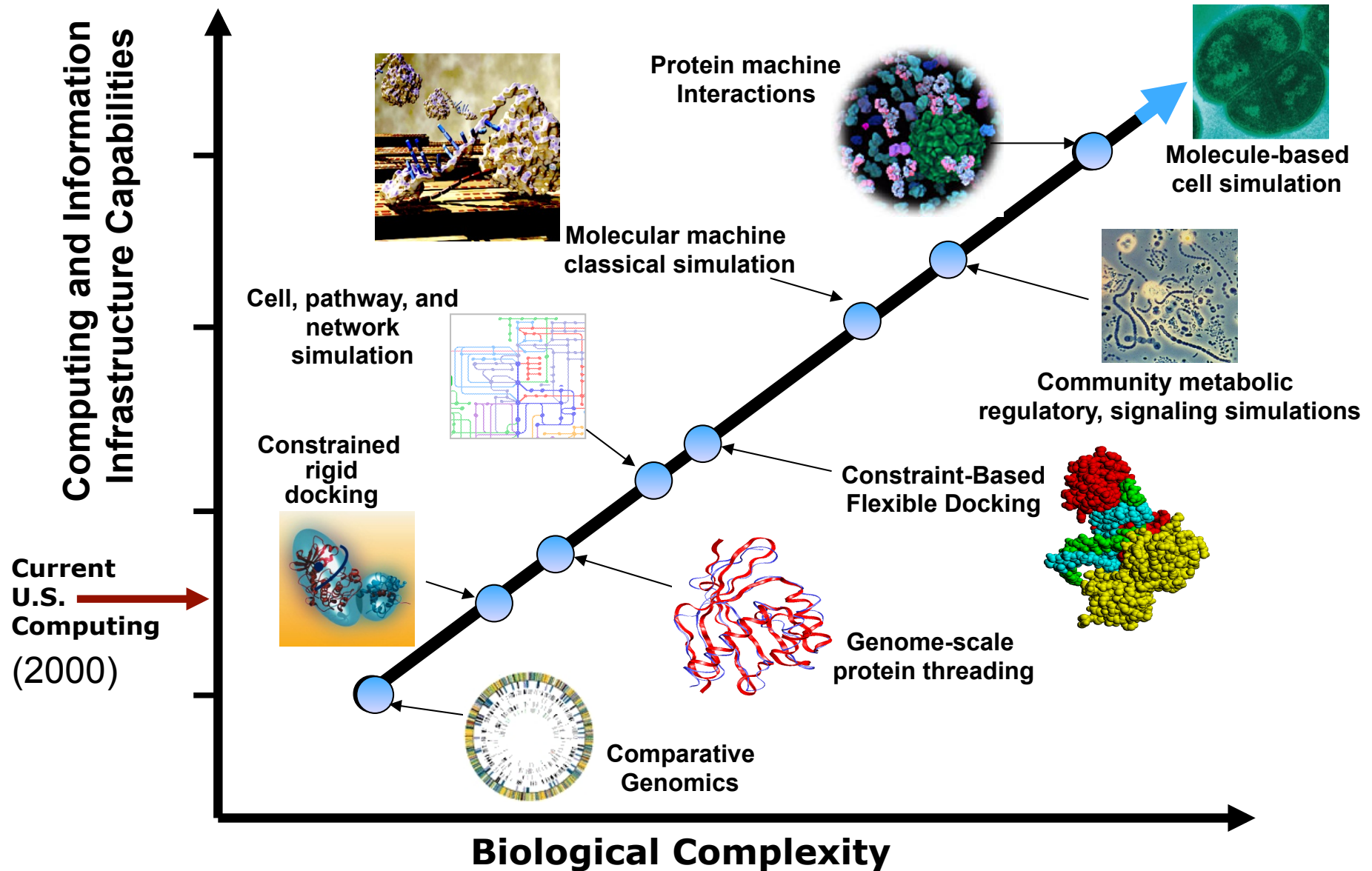
IV Parameter fit through evolutionary algorithm
T. Geyer, X. Mol, S. Blaß & V. Helms (PLoS ONE 2010)

Content of final exam (March 3, 2017)

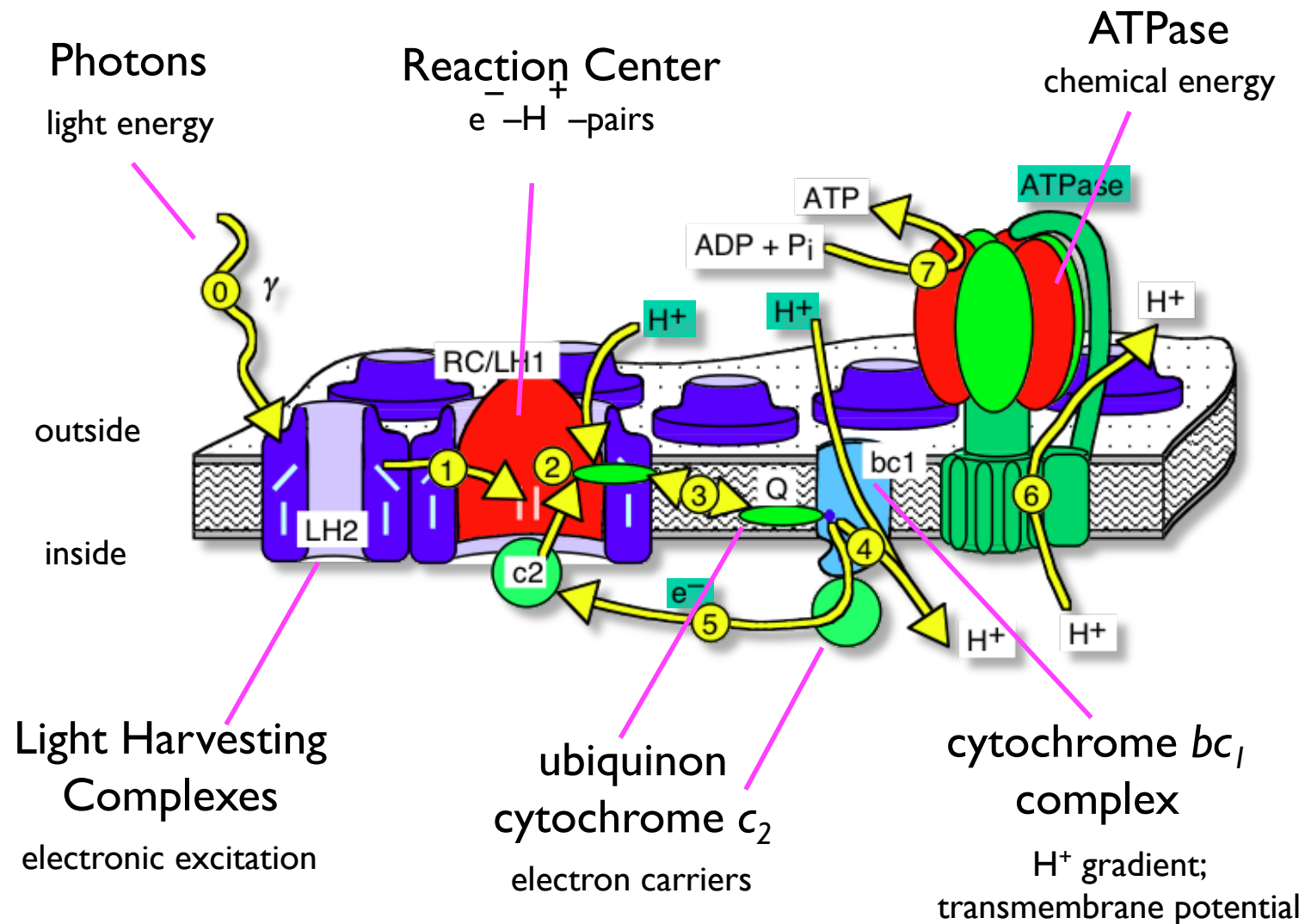
Lecture	Slides relevant for exam
1	18-24
2	1-14, 18-20
3	16-27
4	All
5	1-32
6	24-37
7	None
8	1-18
9	1-15
10	6-18, 30
11	8-33
12	The main ideas of 1-14, 27-43

Lecture	Slides relevant for exam
13	1-30
14	1-19, 25-30, 33, 42
15	2,3, 6-8, 28, 30, 39
16	Main ideas of 1-16
17	1-34
18	1-14
19	18-41
20	17-23
21	None
22	None
23	None
24	None
25	None

“Genomes To Life” Computing Roadmap (NIH/DOE)

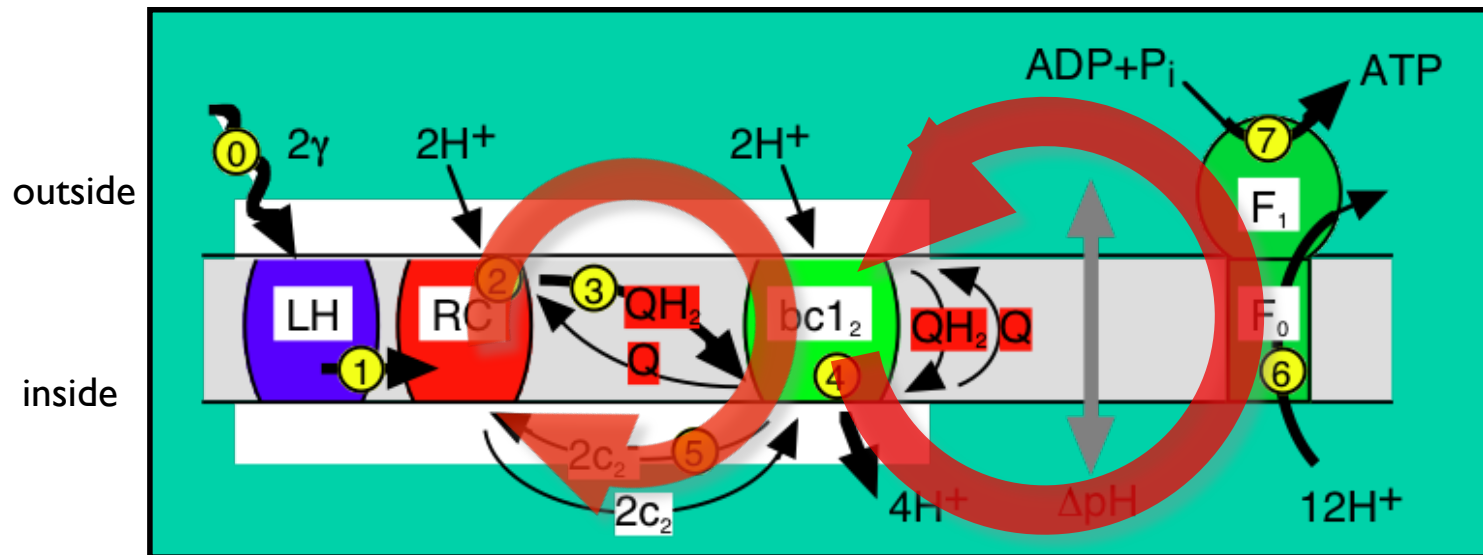
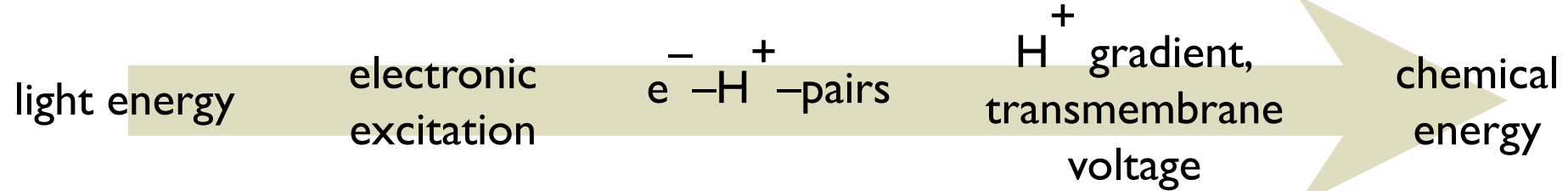


Bacterial Photosynthesis 101



Photosynthesis – cycle view

The conversion chain: stoichiometries must match turnovers!



2 cycles:

electrons

protons

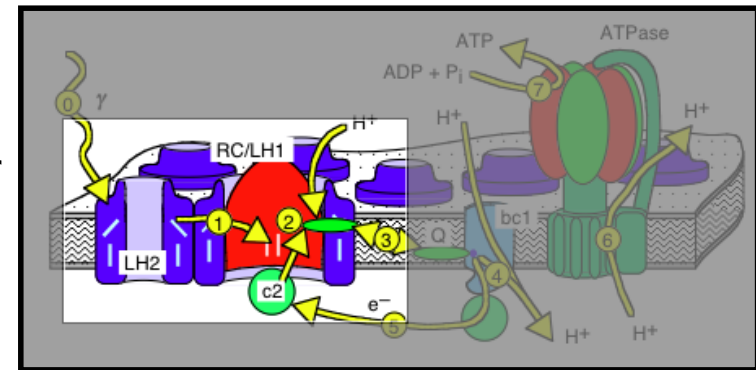
LH1 / LH2 / RC — a la textbook

Collecting photons

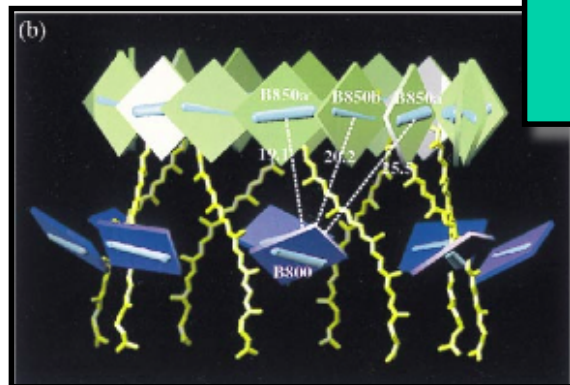
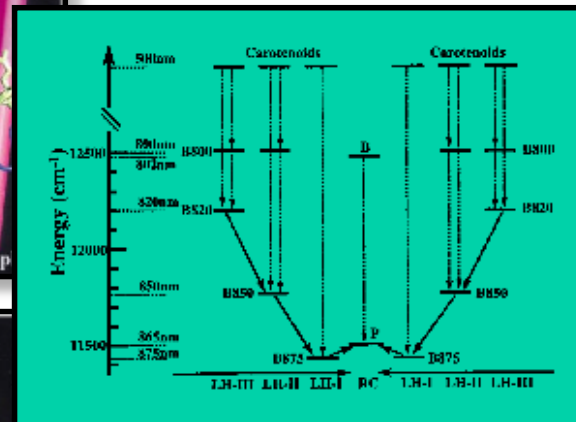
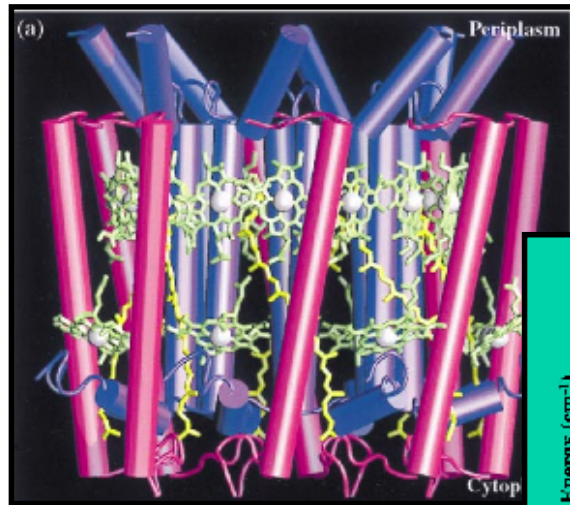
LH2: 8 $\alpha\beta$ dimers

downhill transport of excitons

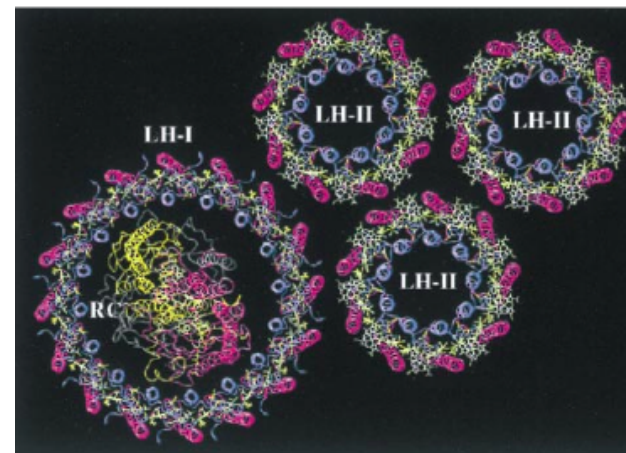
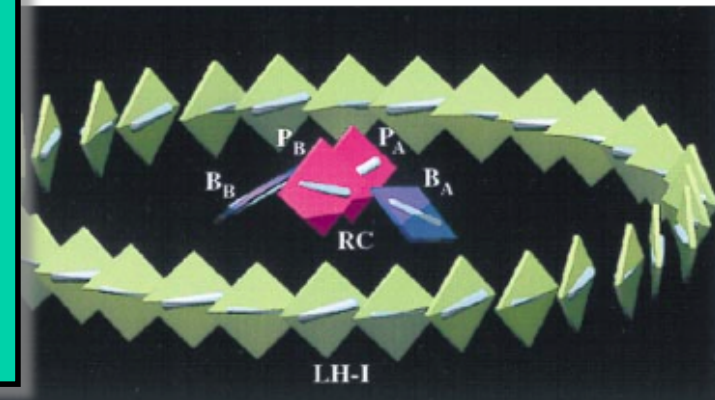
LH2 → LHI → RC



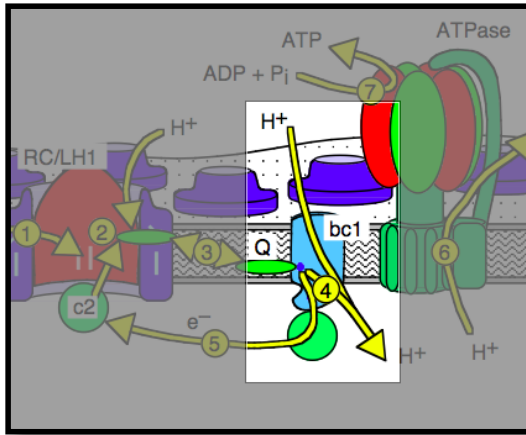
LHI: 16 $\alpha\beta$ dimers



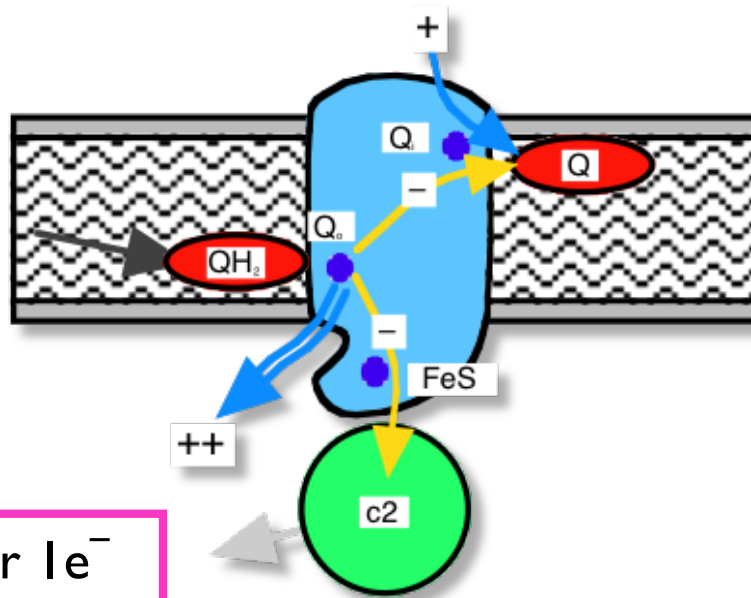
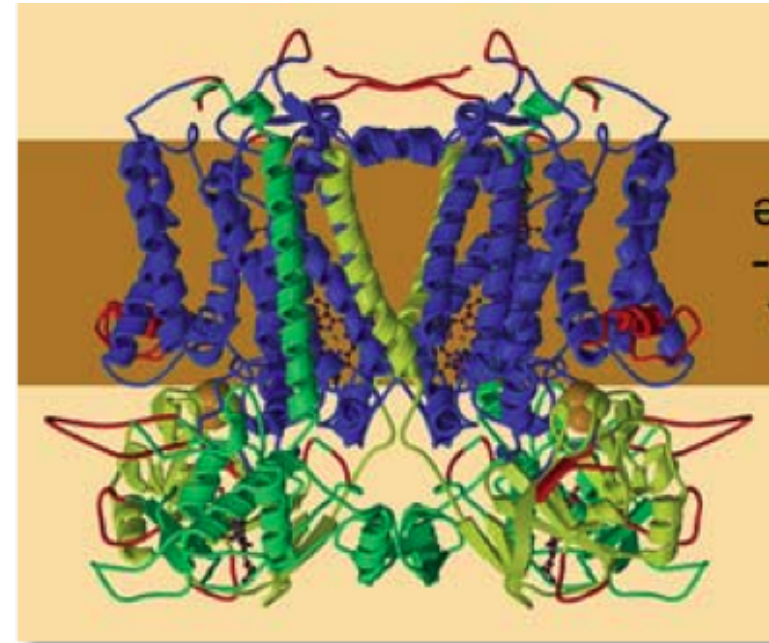
B800, B850, Car.



The Cytochrome *bc*₁ complex



the "proton pump"

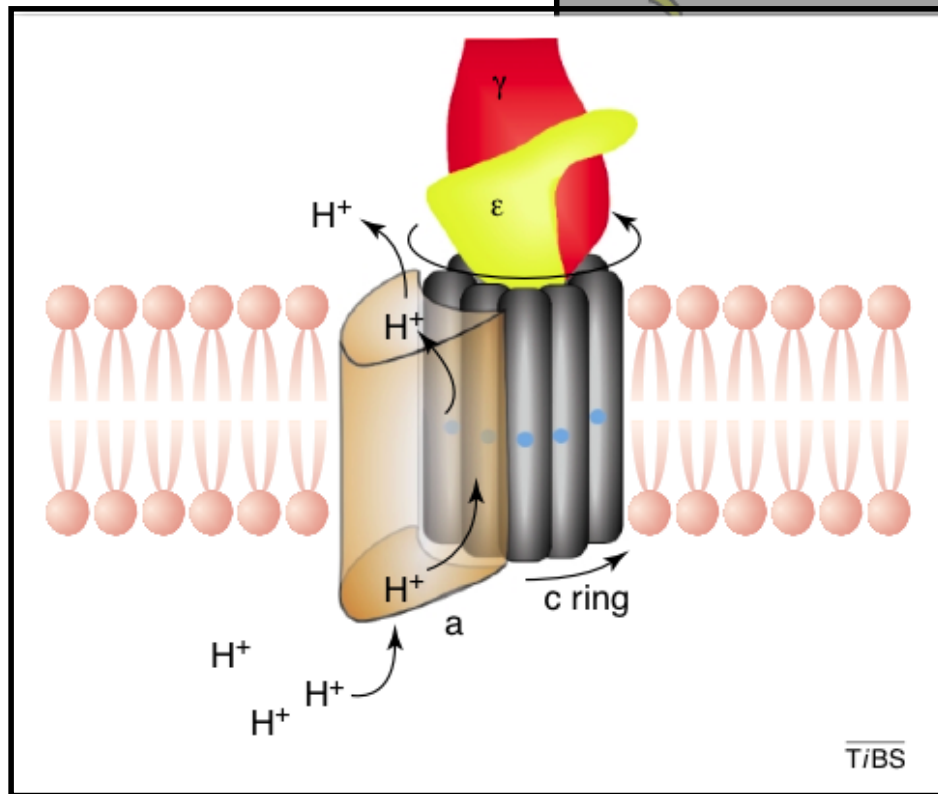
 2H^+ per 1e^- 

Berry, etal, 2004

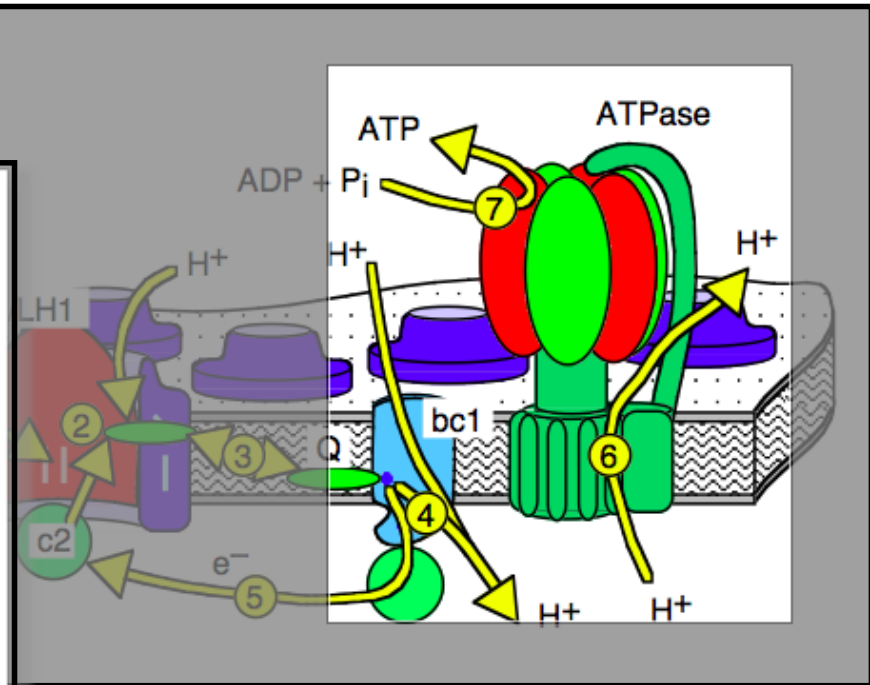
X-ray structures known
always forms a dimer

The F_0F_1 -ATP synthase I

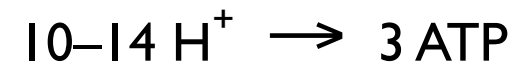
at the end of the chain: producing ATP from the H^+ gradient



Capaldi, Aggeler, 2002



per turn:



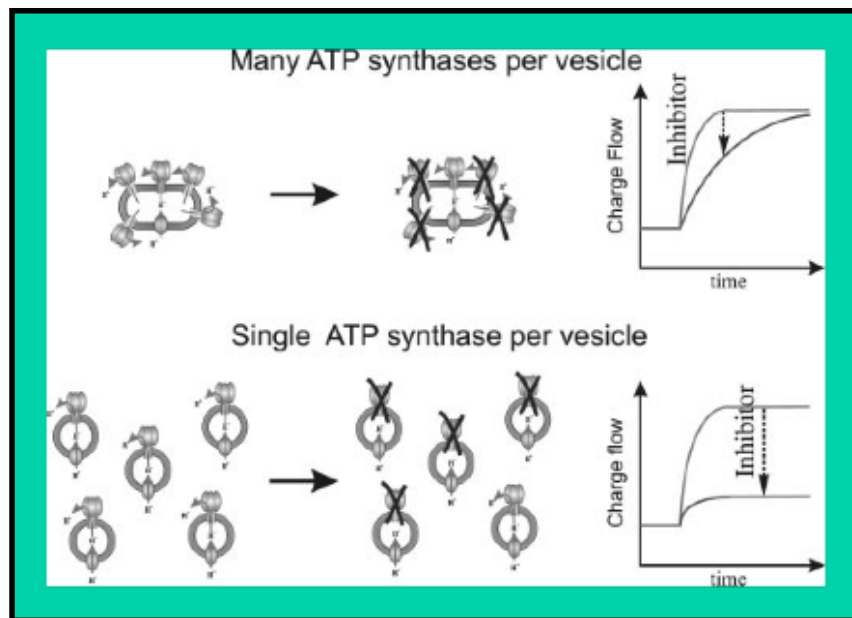
$$1 ATP \triangleq 4 H^+$$

The F_1F_0 -ATP synthase

"...mushroom like structures observed in AFM images..."

➡ ATPase is "visible"

1 ATPase per vesicle

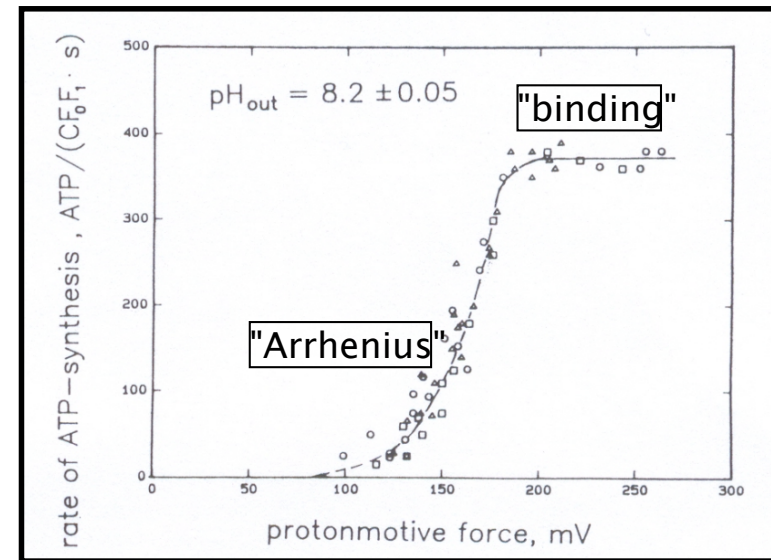


Feniouk et al, 2002

per turn: 10–14 H^+ per 3 ATP

➡ 1 ATP \triangleq 4 H^+

limited throughput of the ATPase



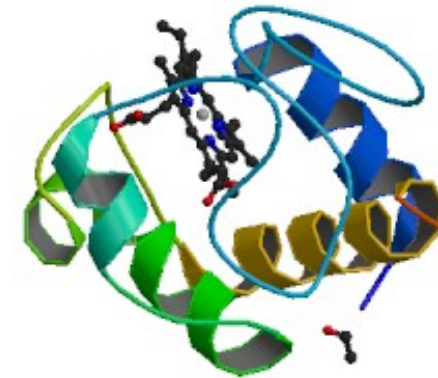
ATPase from	ATP/s	H^+ /s
chloroblasts	<400	1600
E. coli	<100	400

Gräber et al, 1991, 1999

The electron carriers

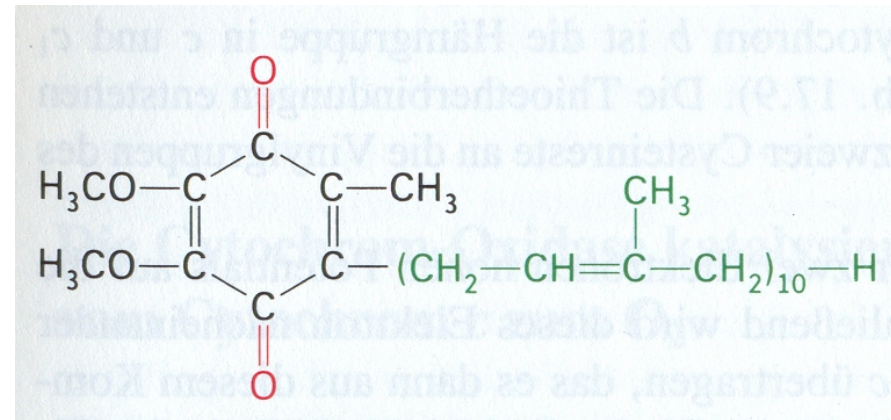
Cytochrome c: carries electrons from bc_1 to R

- heme in a hydrophilic protein shell
- 3.3 nm diameter, water-soluble



Ubiquinone UQ10:
carries electron-proton pairs
from RC to bc_1

- long (2.4 nm)
hydrophobic
isoprenoid tail,
membrane-
soluble

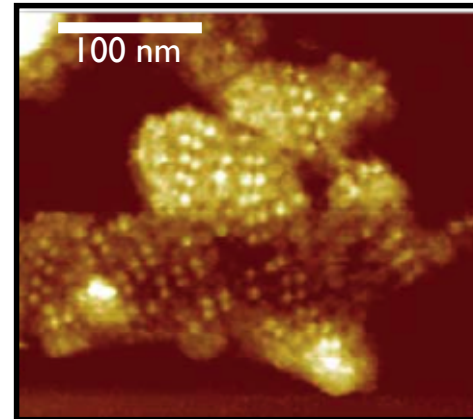
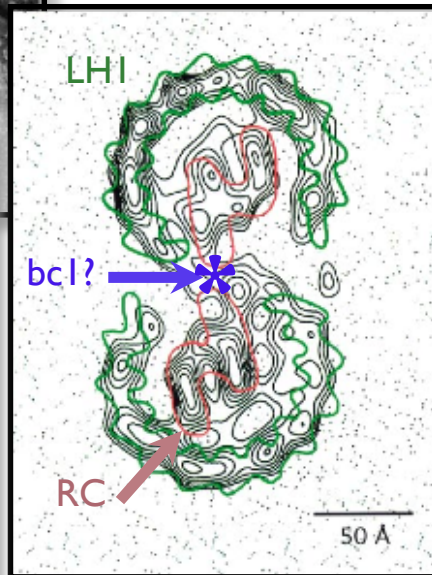
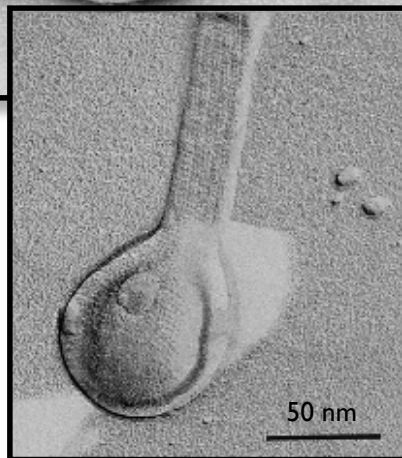
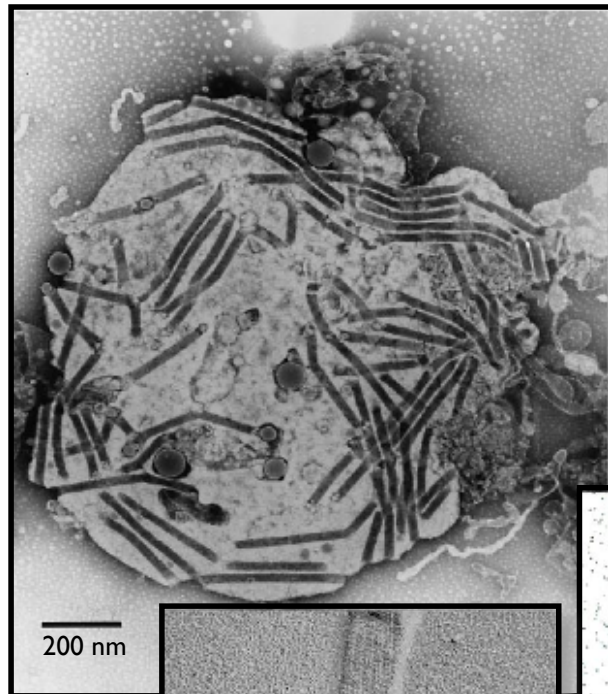


taken from Stryer

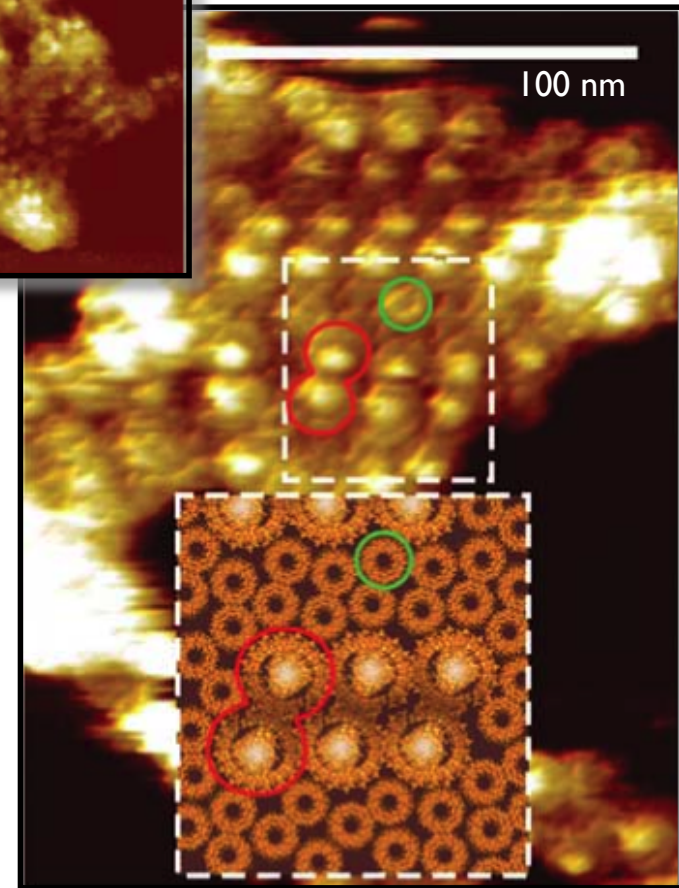
Tubular membranes – photosynthetic vesicles where are the bc_1 complexes and the ATPase?

Jungas et al., 1999

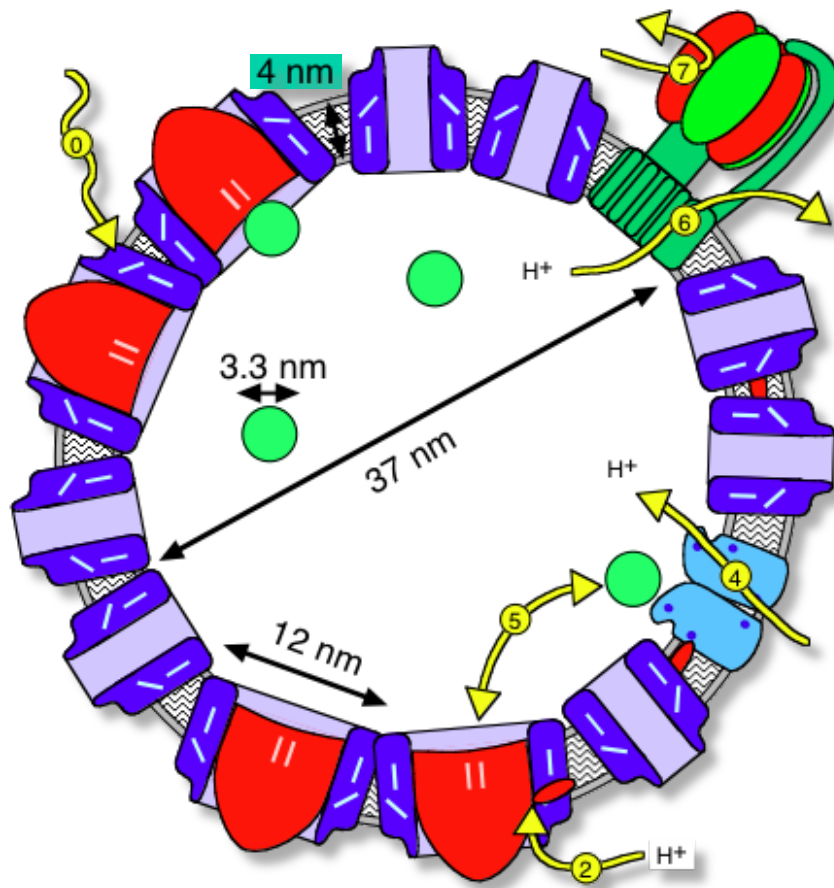
Bahatyrova et al., 2004



no bc_1
found!



Chromatophore vesicle: typical form in *Rh. sphaeroides*



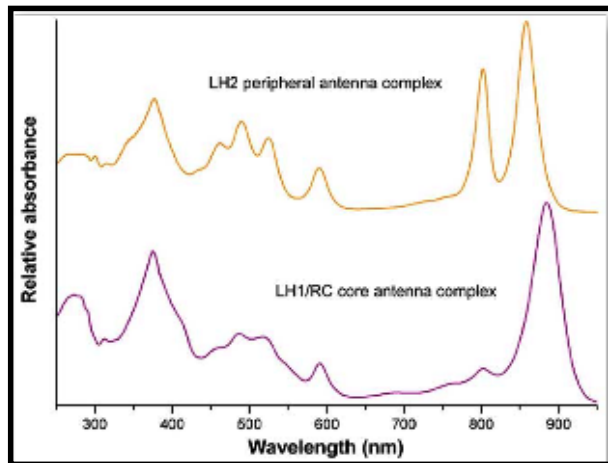
Lipid vesicles
30–60 nm diameter
 H^+ and cyt c inside

average
chromatophore surface
vesicle, 45 nm Ø: 6300 nm²

Vesicles are really small!

Photon capture rate of LHC's

relative absorption spectrum
of LH1/RC and LH2

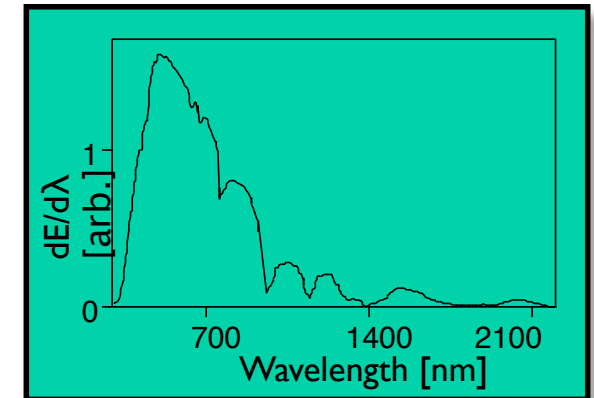


Cogdell et al, 2003

+ Bchl extinction coeff.
normalization ($\sigma_{\text{Bchl}} = 2.3 \text{ \AA}^2$)

Franke, Amesz, 1995

sun's spectrum at ground
(total: 1 kW/m²)



Gerthsen, 1985

multiply

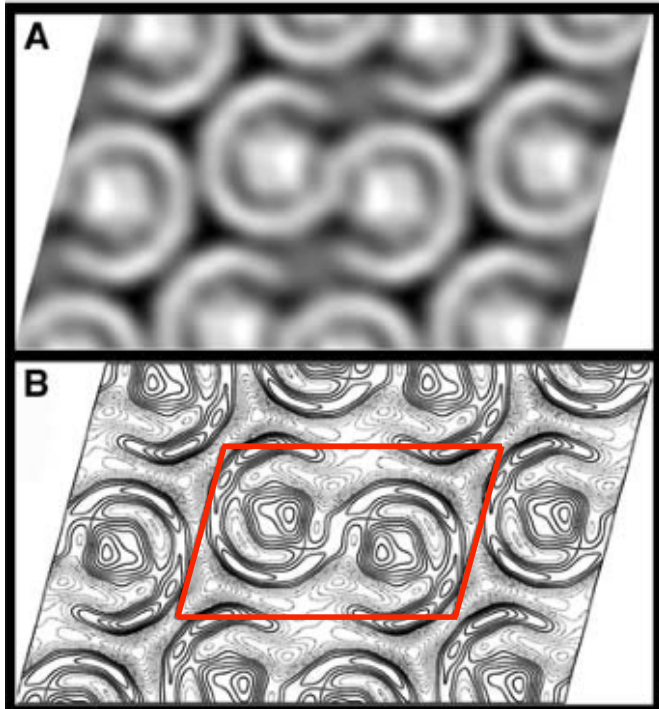
capture rate: $0.1 \frac{\gamma}{\text{s kW Bchl}}$

typical growth condition:
18 W/m² Feniouk et al, 2002

LH1: 16 * 3 Bchl ➡ 14 γ/s
LH2: 10 * 3 Bchl ➡ 10 γ/s

LH1 / LH2 / RC — native

electron micrograph
and density map



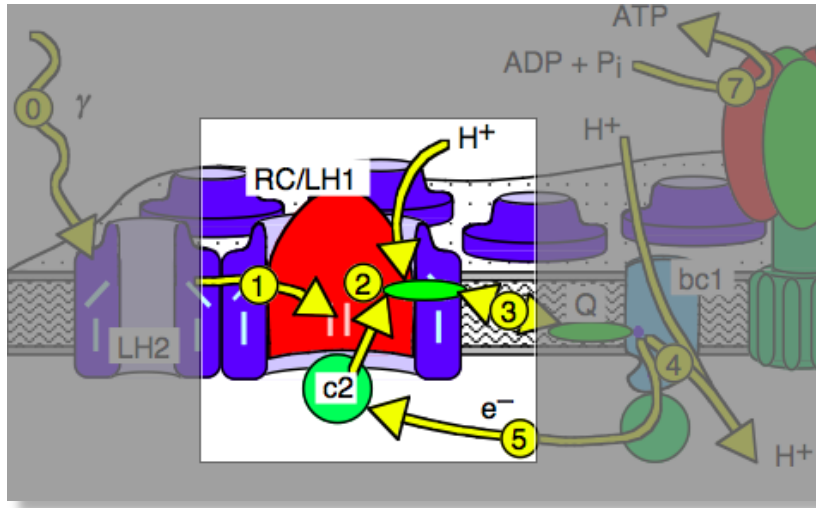
Siebert et al, 2004
125 * 195 Å², $\gamma = 106^\circ$

	Area per:	per vesicle (45 nm)
LH1 monomer (hexagonal)	146 nm ²	
LH1 dimer	234 nm ²	
LH2 monomer	37 nm ²	
LH1 ₂ + 6 LH2	456 nm ²	11

Chromatophore surface
vesicle, 45 nm Ø: 6300 nm²

Photon processing rate at the RC

Which process limits the RCs turnover?



Unbinding of the quinol

➡ 25 ms Milano et al. 2003

+ binding, charge transfer
 ≈ 50 ms per quinol (estimate)

with $2e^- H^+$ pairs per quinol

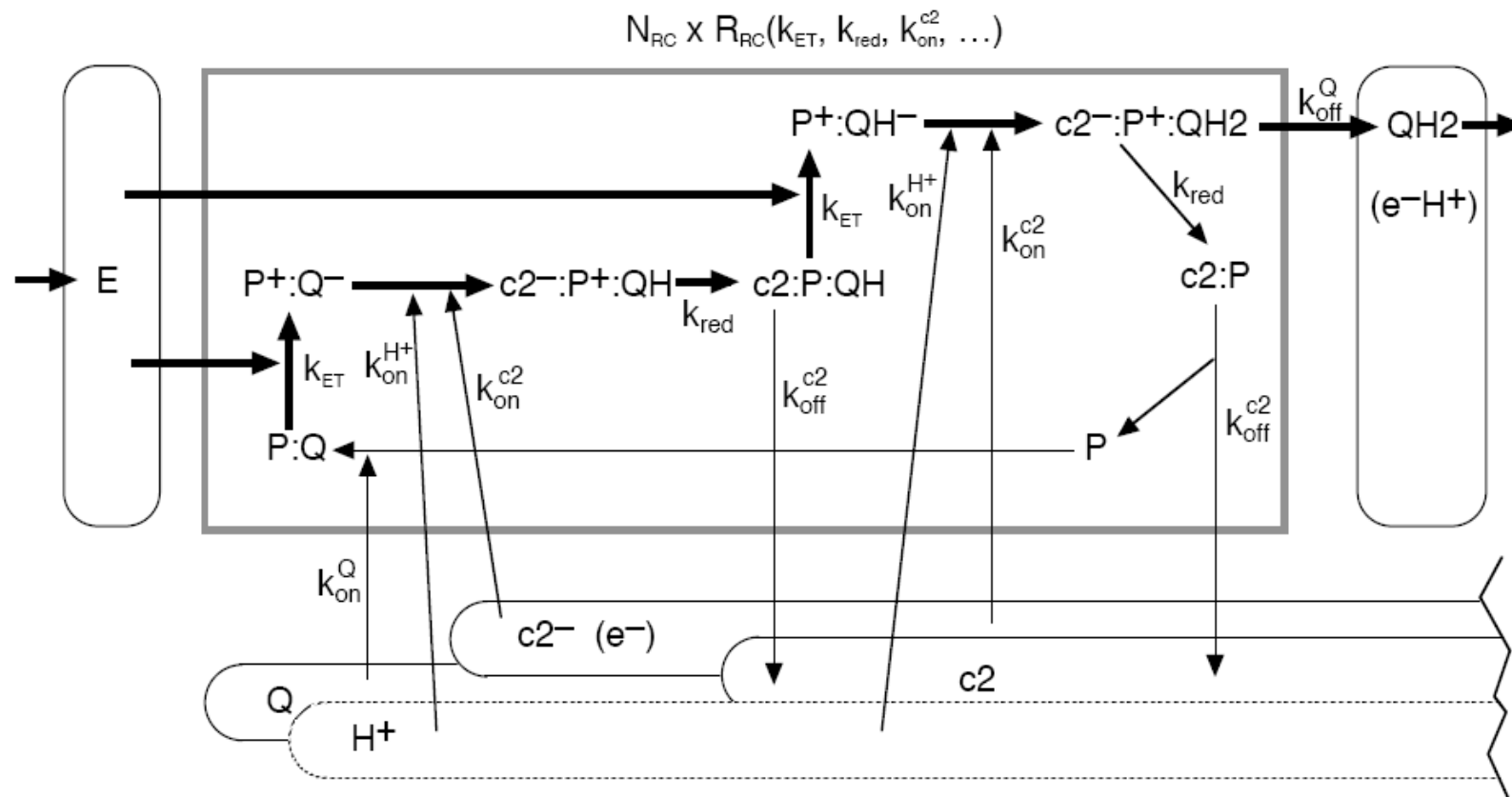
➡ 40–50 γ/s per RC
 ≈ 22 QH_2/s

I RC can serve
 I LHI
 + 3 LH2
 = 44 γ/s

$LHI_2 + 6 LH2 \triangleq 456 \text{ nm}^2 \rightarrow$ II LHI dimers including 22 RCs
 on one vesicle

➡ 480 Q/s can be loaded @ 18 W/m^2 per vesicle

Modelling of internal processes at reaction center



All individual reactions with their individual rates k together determine the overall conversion rate R_{RC} of a single RC.

Thick arrows : flow of the energy from the excitons through the cyclic charge state changes of the special pair Bchl (P) of the RC.

Rounded rectangles : reservoirs

***bc*₁ Placement — Diffusional limits?**

Roundtrip times

maximal capacity of the carriers:

$$T = T_{RC} + T_{bcl} + T_{Diff}$$

Cytochrome *c*₂:

$$T_{RC} \approx 1 \text{ ms}$$

$$T_{bcl} \approx 12 \text{ ms}$$

$$T_{Diff} \approx 3 \mu\text{s}$$

$T_{\text{round-trip}} = 13 \text{ ms} \Rightarrow \leq 3 \text{ cyt } c \text{ per vesicle}$
sufficient to carry e^- 's
available: 22 cyt *c* per vesicle

Quinol:

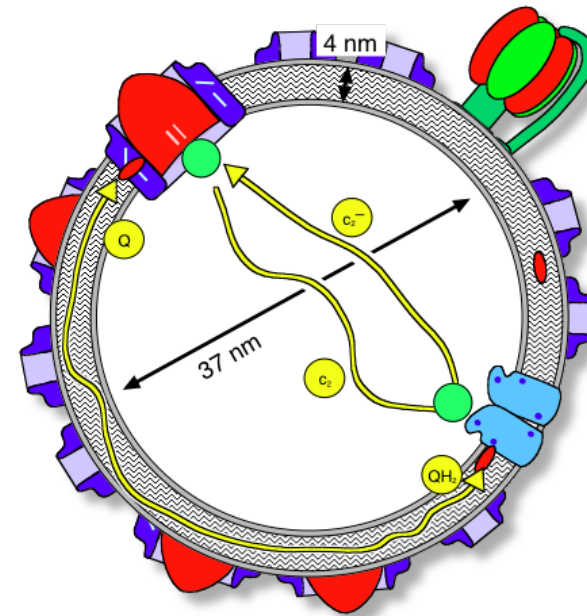
$$T_{RC} \approx 50 \text{ ms}$$

$$T_{bcl} \approx 23 \text{ ms}$$

$$T_{Diff} \approx 1 \text{ ms}$$

$T_{\text{round-trip}} = 75 \text{ ms} \Rightarrow \leq 7 \text{ Q per vesicle}$
sufficient to carry e^- 's.

available: 100 Q per vesicle

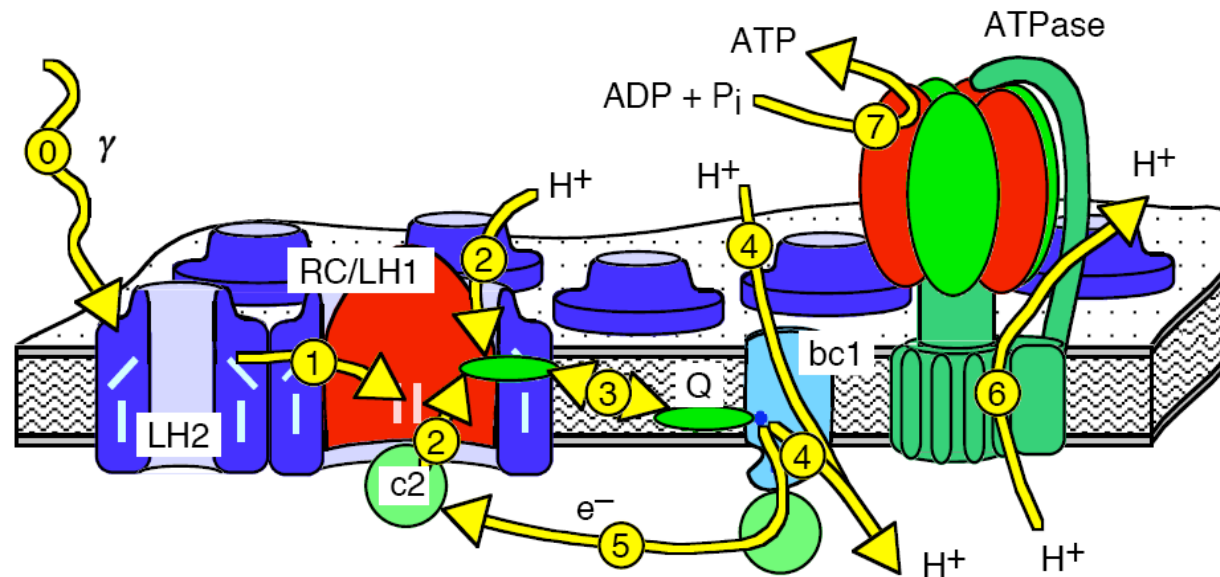


Diffusion is not limiting

③ poses no constraints
on the position of *bc*₁

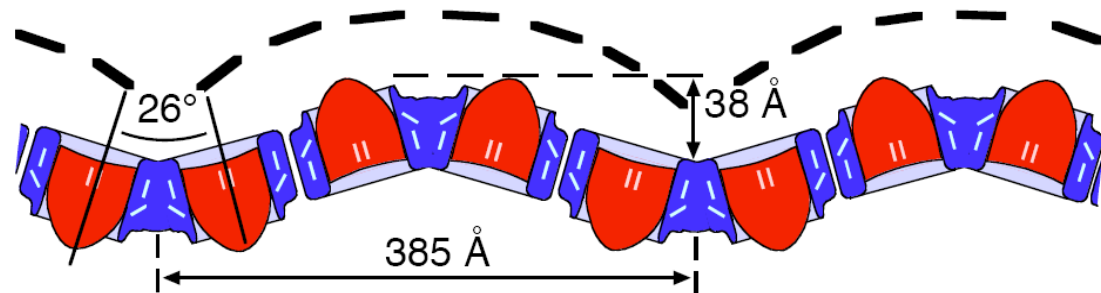
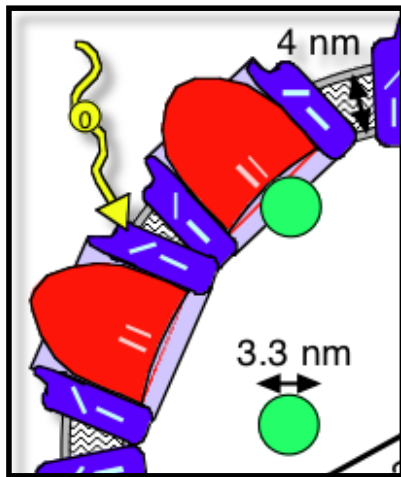
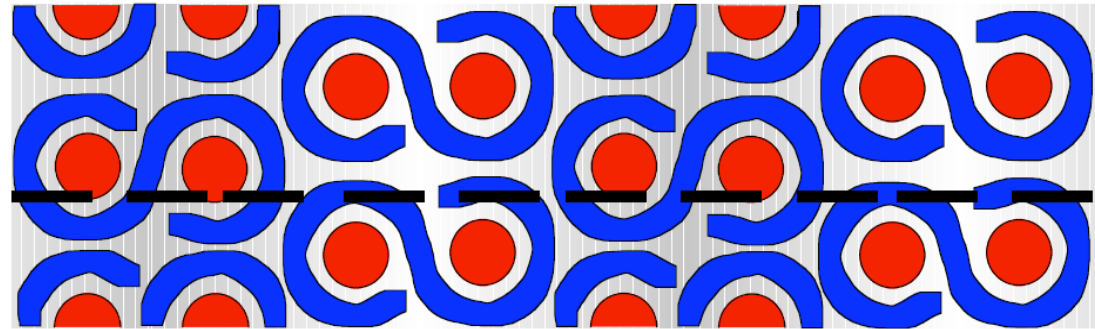
Parameters

protein	throughput per protein (natural units)	H ⁺ equivalents per protein [1/s]	total number per avg. vesicle of 45 nm diameter	rate determined from	explained in section
LH2	10 γ/s	20	60	absorption spectra +	III A
LH1 dimer	$2 \times 14 \gamma/s$	56	10	+ light intensity of 18 W/m ²	III A
RC	22 QH2/s	88	20	QH2 (un)binding	III B
bc1 dimer	$\leq 2 \times 42 c2/s$	168	3 (... 10)	measured activity at $\Delta pH = 0$	III C
ATPase	$\leq 100 \text{ ATP/s}$	400	1	measured throughput	III D
cytochrome <i>c</i> ₂	80 e ⁻ /s	160	20	(un)binding at the bc1	V A (III B, III C)
ubiquinone	$10 \times 2(e^- H^+)/s$	40	100	(un)binding at the RC and the bc1	V A (III B, III C)



reconstituted LH1 dimers in planar lipid membranes explain intrinsic curvature of vesicles

Drawn after AFM images of Scheuring *et al* of LH1 dimers reconstituted into planar lipid membranes.



Values fit nicely to the proposed arrangement of LH1 dimers, when one assumes that they are stiff enough to retain the bending angle of 26° that they would have on a spherical vesicle of 45 nm diameter and taking into account the length of a single LH1 dimer of about 19.5 nm.

Proposed setup of a chromatophore vesicle

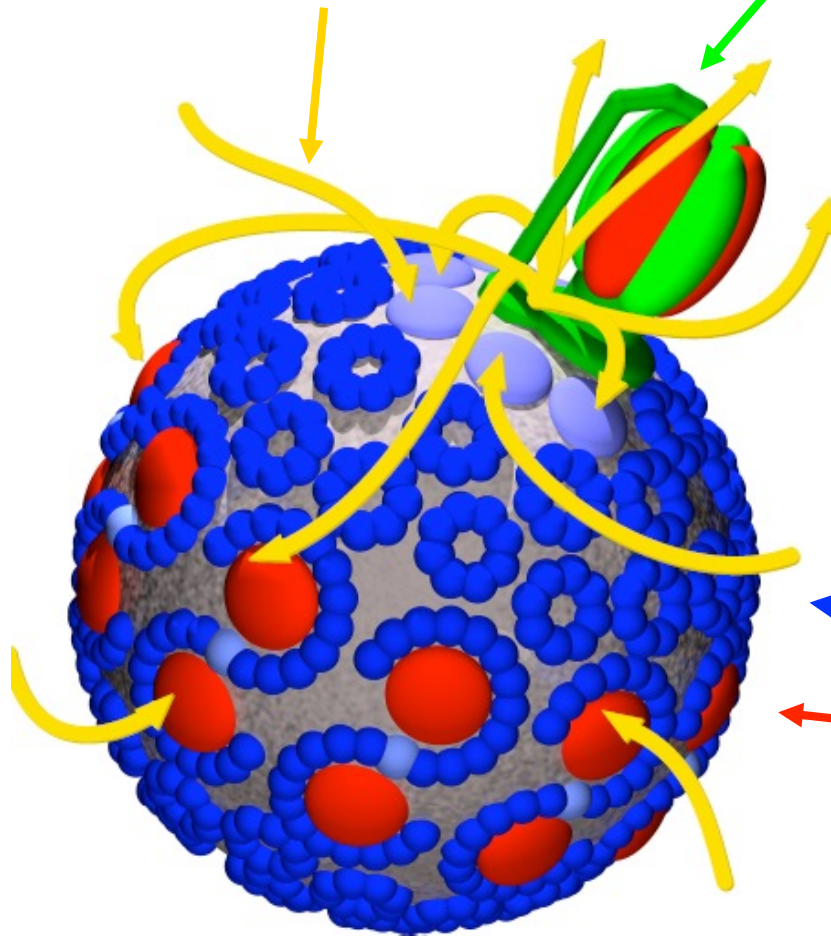
yellow arrows: diffusion of the protons out of the vesicle via the ATPase and to the RCs and bc1s.

At the „poles“

green/red: the ATPase

light blue: the bc1 complexes

Increased proton density close to the ATPase suggests close proximity of ATPase and bc_1 complexes.



blue: small LH2 rings (blue)

blue/red: Z-shaped LH1/RC dimers form a linear array around the “equator” of the vesicle, determining the vesicle’s diameter by their intrinsic curvature.

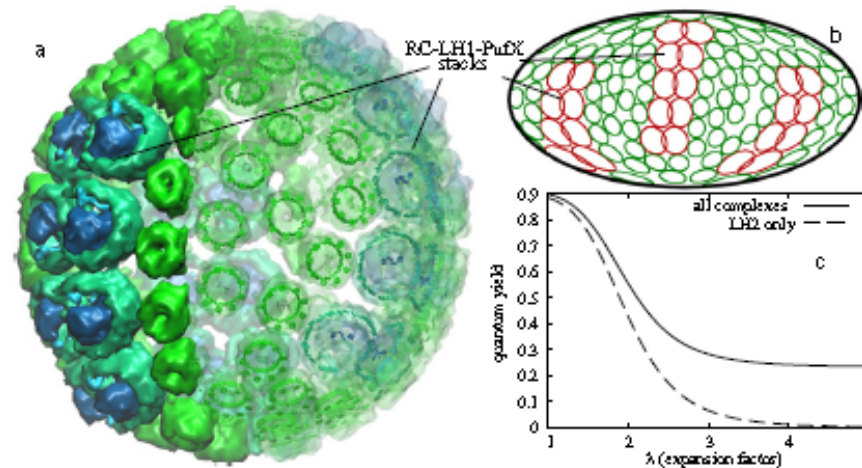
Summary

Integrated model of binding + photophysical + redox processes
inside of chromatophore vesicles

Various experimental data
fit well together

Equilibrium state.

How to model
non-equilibrium processes?



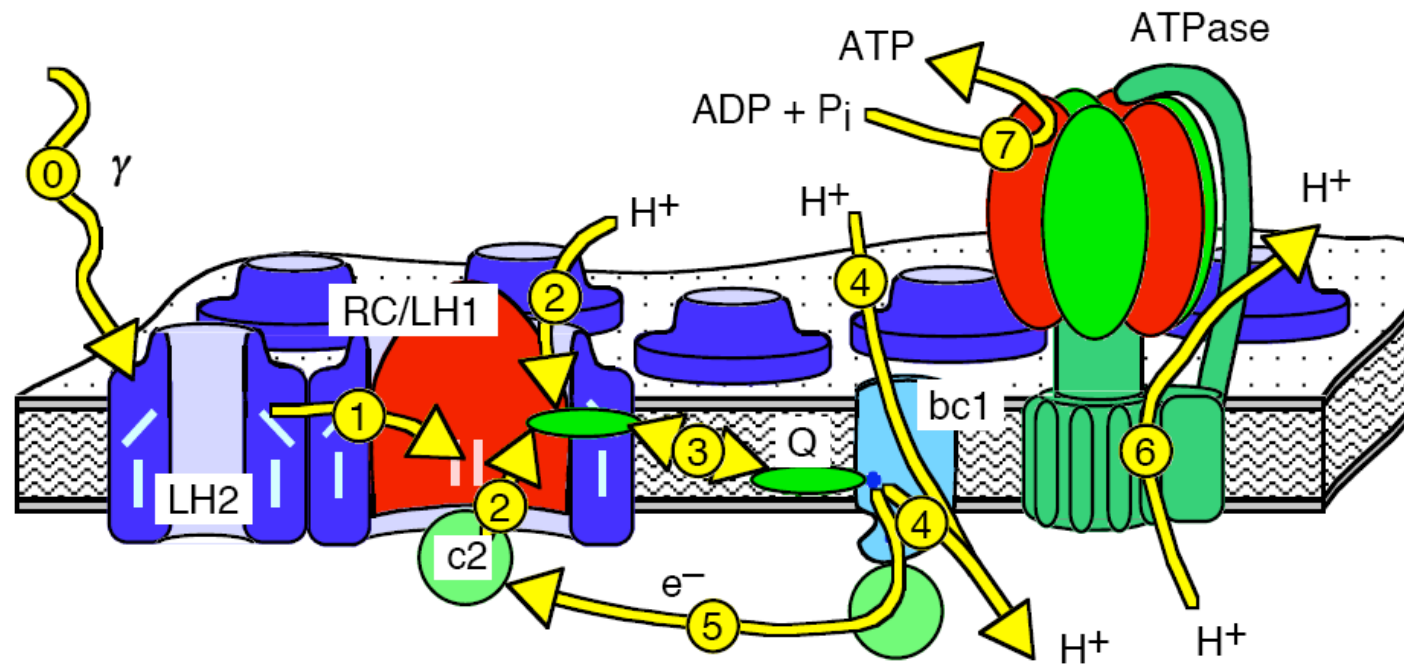
Biophysical Journal Volume 99 July 2010 67–75

67

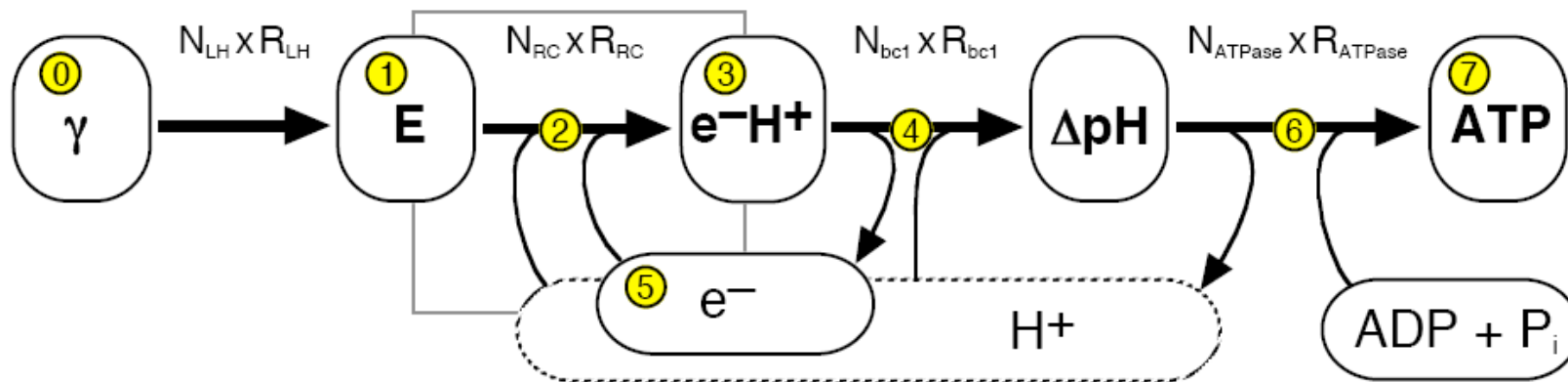
Photosynthetic Vesicle Architecture and Constraints on Efficient Energy Harvesting

Melih Şener,^{†‡} Johan Strümpfer,^{†§} John A. Timney,[¶] Arvi Freiberg,^{||} C. Neil Hunter,[¶] and Klaus Schulten^{†‡§*}
[†]Beckman Institute for Advanced Science and Technology, [‡]Department of Physics, and [§]Center for Biophysics and Computational Biology, University of Illinois at Urbana-Champaign, Urbana, Illinois; [¶]Department of Molecular Biology and Biotechnology, University of Sheffield, Sheffield, United Kingdom; and ^{||}Institute of Physics and ^{**}Institute of Molecular and Cell Biology, University of Tartu, Tartu, Estonia

Photosynthesis: textbook view



Viewing the photosynthetic apparatus as a conversion chain



Thick arrows : path through which the photon energy is converted into chemical energy stored in ATP via the intermediate stages (rounded rectangles).

Each conversion step takes place in parallelly working proteins. Their number N times the conversion rate of a single protein R determines the total throughput of this step.

γ : incoming photons collected in the LHCs

E : excitons in the LHCs and in the RC

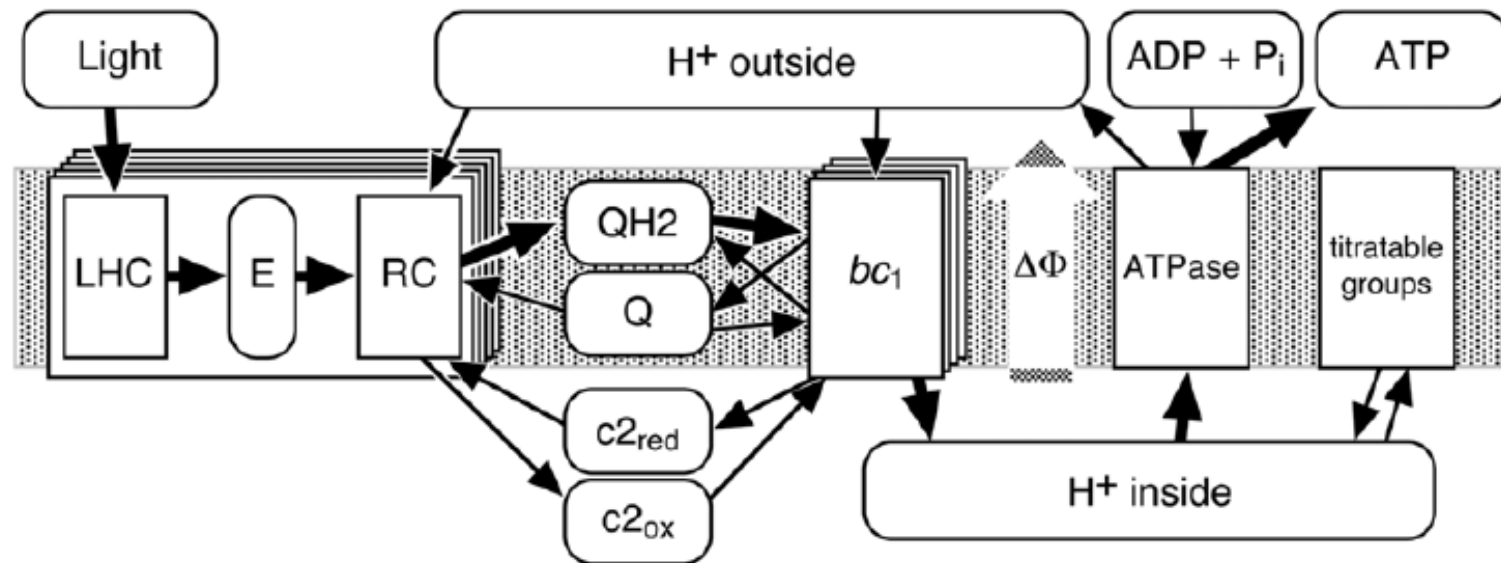
e^-H^+ electron-proton pairs stored on the quinols

e^- for the electrons on the cytochrome c_2

pH : transmembrane proton gradient

H^+ : protons outside of the vesicle (broken outline of the respective reservoir).

Stochastic dynamics simulations: Molecules & Pools model



Round edges: **pools** for metabolite molecules

Rectangles: protein machines are modeled explicitly as multiple copies

fixed set of parameters

integrate rate equations with stochastic algorithm

Stochastic simulations of cellular signalling

Traditional computational approach to chemical/biochemical kinetics:

- (a) start with a set of coupled **ODEs** (reaction rate equations) that describe the time-dependent concentration of chemical species,
- (b) use some **integrator** to calculate the concentrations as a function of time given the rate constants and a set of initial concentrations.

Successful **applications** : studies of yeast cell cycle, metabolic engineering, whole-cell scale models of metabolic pathways (E-cell), ...

Major problem: cellular processes occur in very small volumes and frequently involve **very small number of molecules**.

E.g. in gene expression processes a few TF molecules may interact with a single gene regulatory region.

E.coli cells contain on average only 10 molecules of Lac repressor.

Include stochastic effects

(Consequence1) → modeling of reactions as continuous fluxes of matter is no longer correct.

(Consequence2) Significant **stochastic fluctuations** occur.

To study the stochastic effects in biochemical reactions, stochastic formulations of chemical kinetics and Monte Carlo computer simulations have been used.

Daniel Gillespie (J Comput Phys 22, 403 (1976); J Chem Phys 81, 2340 (1977)) introduced the exact **Dynamic Monte Carlo (DMC)** method that connects the traditional chemical kinetics and stochastic approaches.

Basic outline of the direct method of Gillespie

(Step i) generate a list of the components/species and define the initial distribution at time $t = 0$.

(Step ii) generate a list of possible events E_i (chemical reactions as well as physical processes).

(Step iii) using the current component/species distribution, prepare a probability table $P(E_i)$ of all the events that can take place.

Compute the total probability

$$P_{tot} = \sum P(E_i)$$

$P(E_i)$: probability of event E_i .

(Step iv) Pick two random numbers r_1 and $r_2 \in [0...1]$ to decide which event E_μ will occur next and the amount of time τ after which E_μ will occur.

Basic outline of the direct method of Gillespie

Using the random number r_1 and the probability table, the event E_μ is determined by finding the event that satisfies the relation

$$\sum_{i=1}^{\mu-1} P(E_i) < r_1 P_{tot} \leq \sum_{i=1}^{\mu} P(E_i)$$

The second random number r_2 is used to obtain the amount of time τ between the reactions

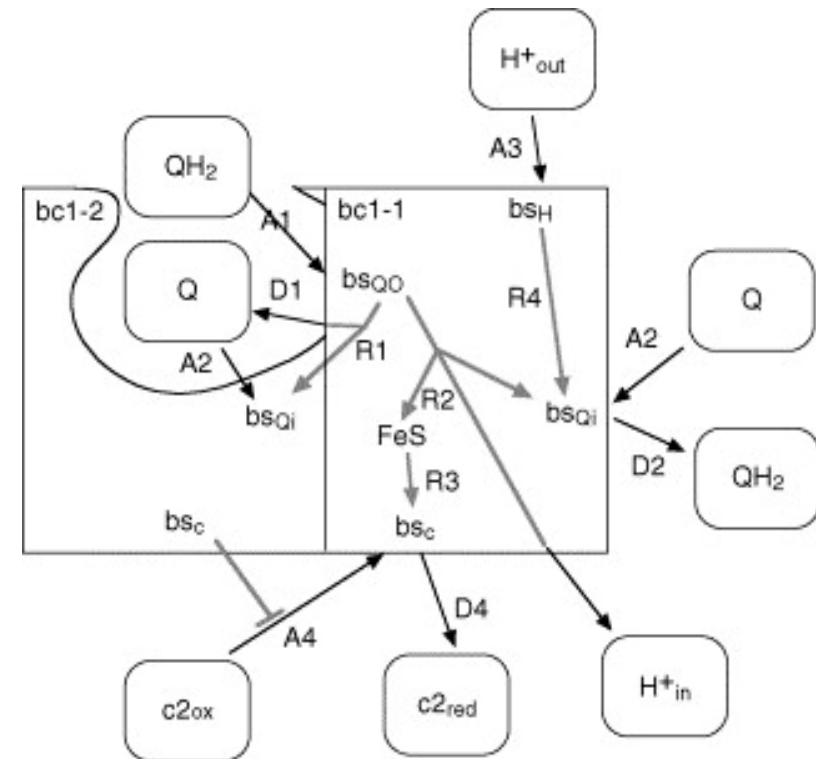
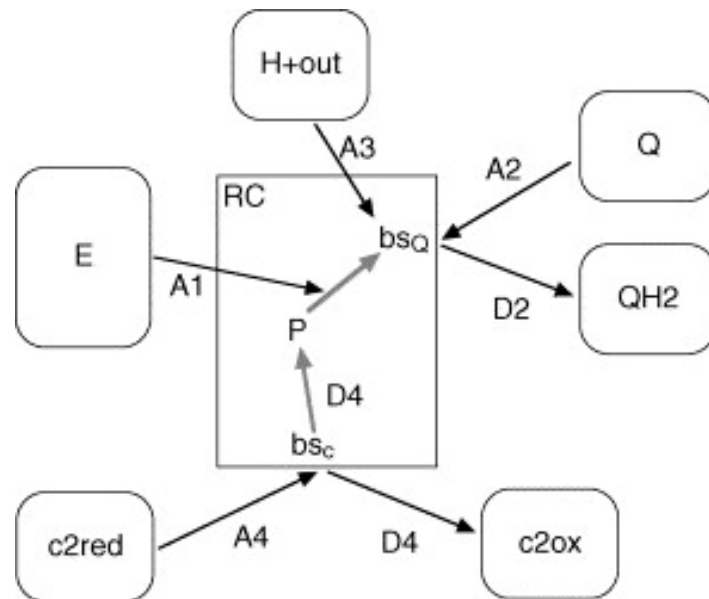
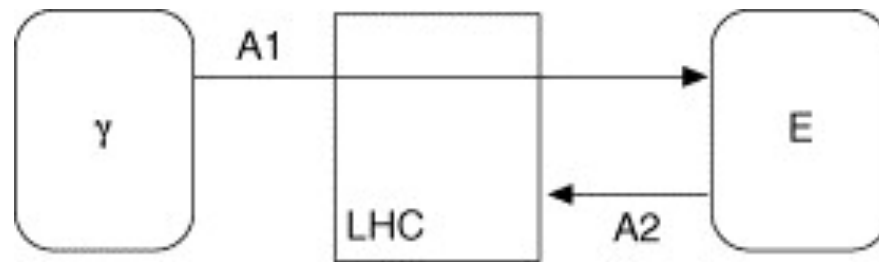
$$\tau = -\frac{1}{P_{tot}} \ln(r_2)$$

As the total probability of the events changes in time, the time step between occurring steps varies.

Steps (iii) and (iv) are repeated at each step of the simulation.

The necessary number of runs depends on the inherent noise of the system and on the desired statistical accuracy.

reactions included in stochastic model of chromatophore



Stochastic simulations of a complete vesicle

Model vesicle: 12 LH1/RC-monomers
 1-6 bc_1 complexes
 1 ATPase

 120 quinones
 20 cytochrome c_2

integrate rate equations with:

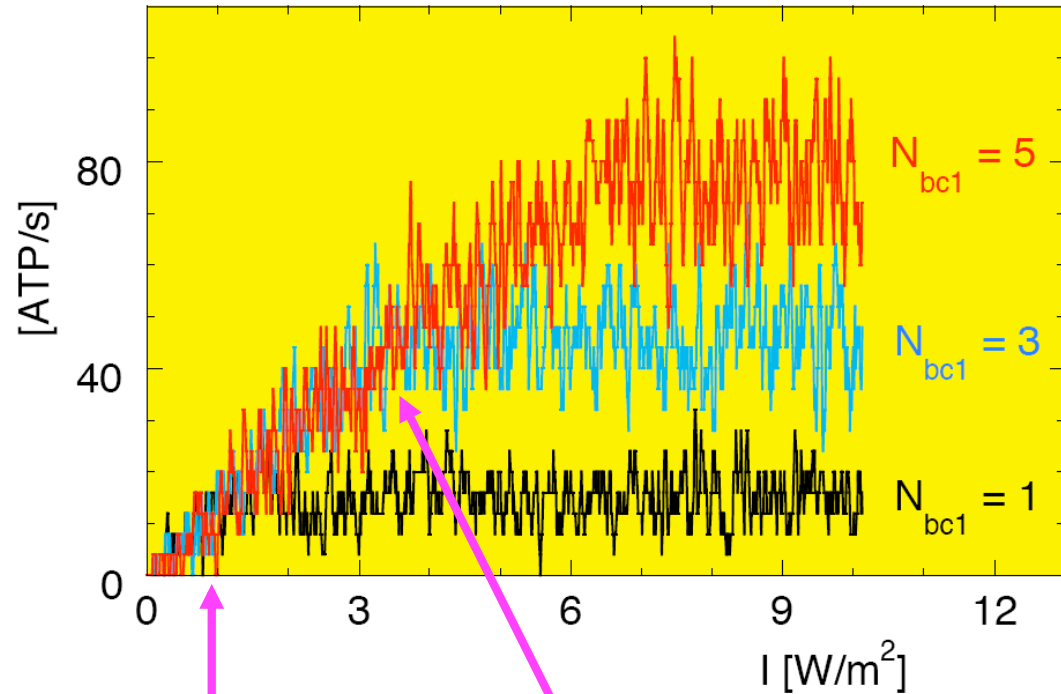
- Gillespie algorithm (associations)
- Timer algorithm (reactions); 1 random number determines when reaction occurs

simulating 1 minute real time requires 1.5 minute on one opteron 2.4 GHz proc

simulate increase of light intensity (sunrise)

during 1 minute,
light intensity is slowly
increased from 0 to 10 W/m²
(quasi steady state)

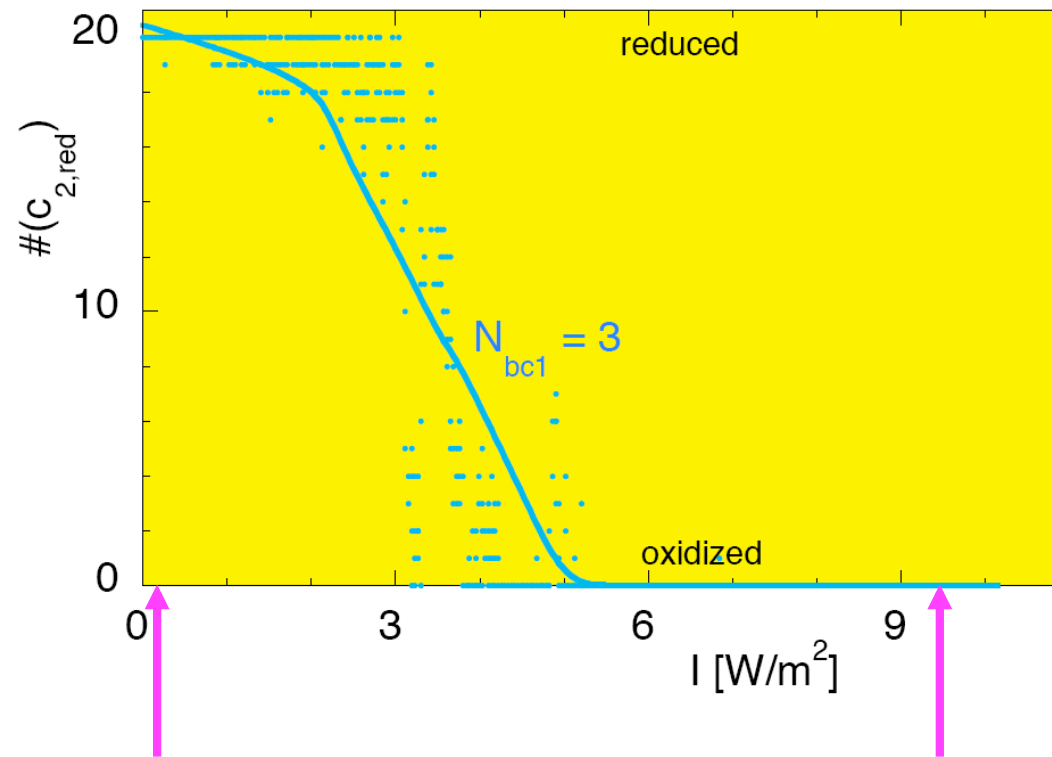
- there are two regimes
- one limited by available light
 - one limited by bc₁ throughput



low light intensity:
linear increase of
ATP production
with light intensity

high light intensity:
saturation is reached
the later the higher the
number of bc₁ complexes

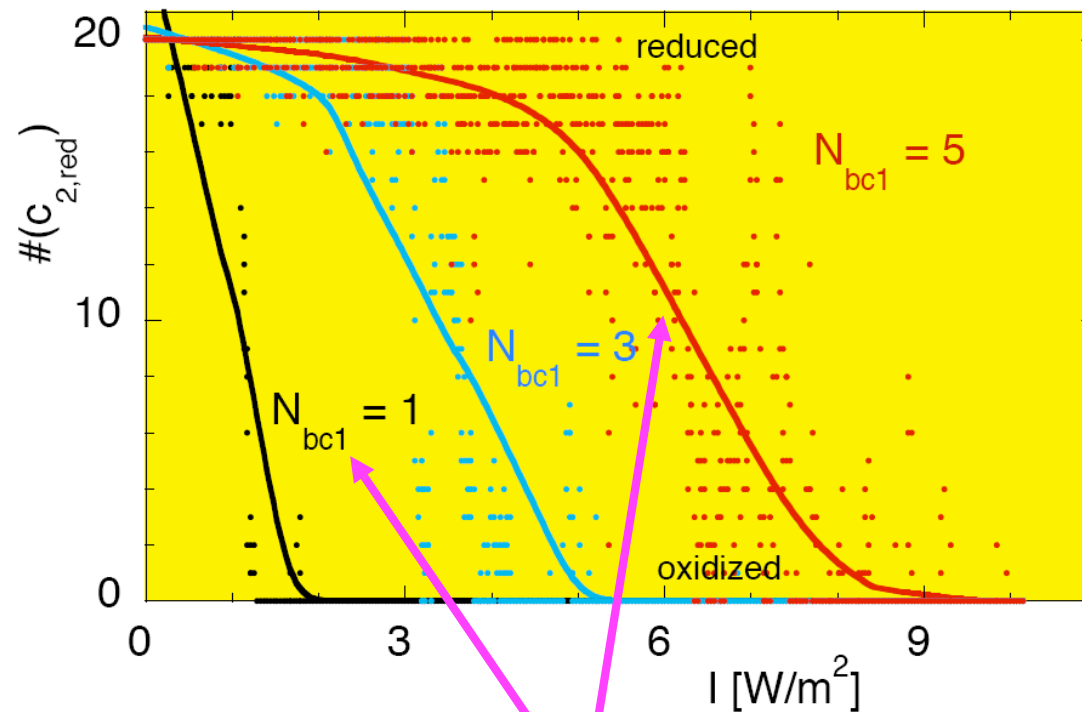
oxidation state of cytochrome c_2 pool



low light intensity:
all 20 cytochrome c_2
are reduced by bc_1

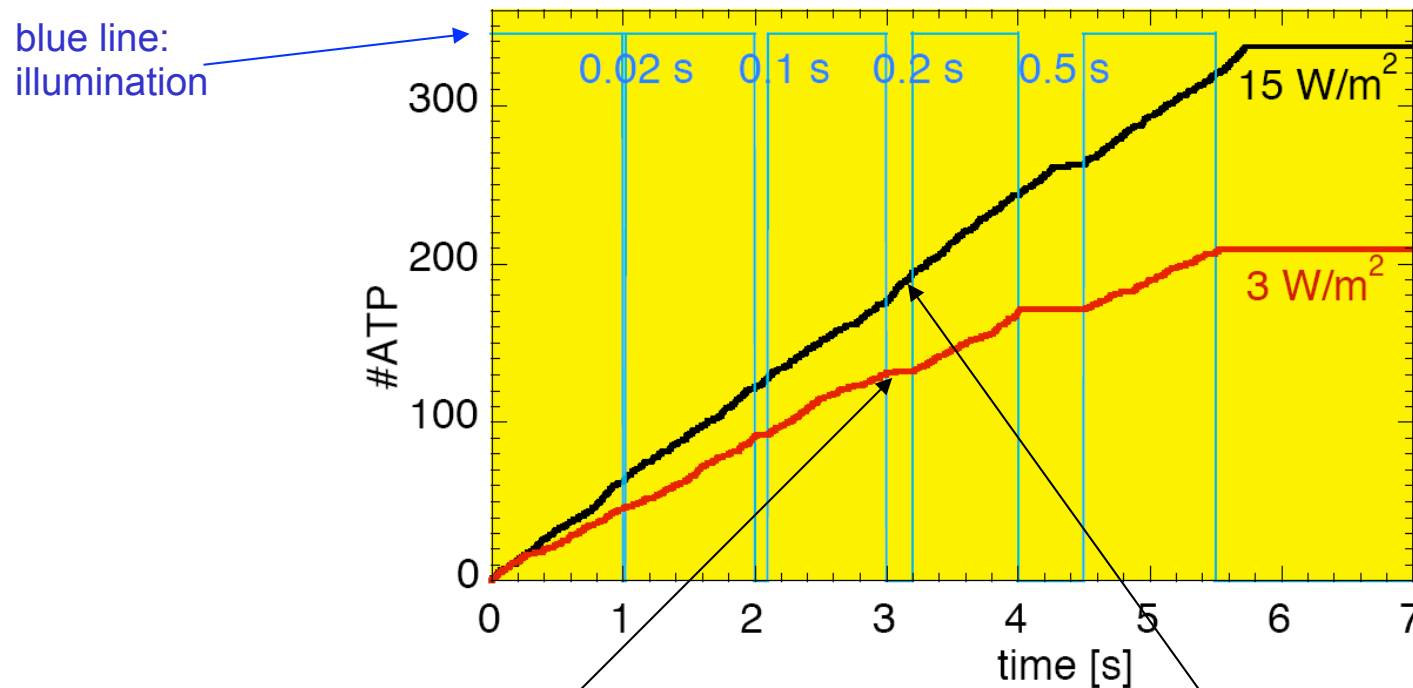
high light intensity
 RCs are faster than bc_1 ,
 c_2 s wait for electrons

oxidation state of cytochrome c_2 pool



more bc_1 complexes
can load more
cytochrome c_2 s

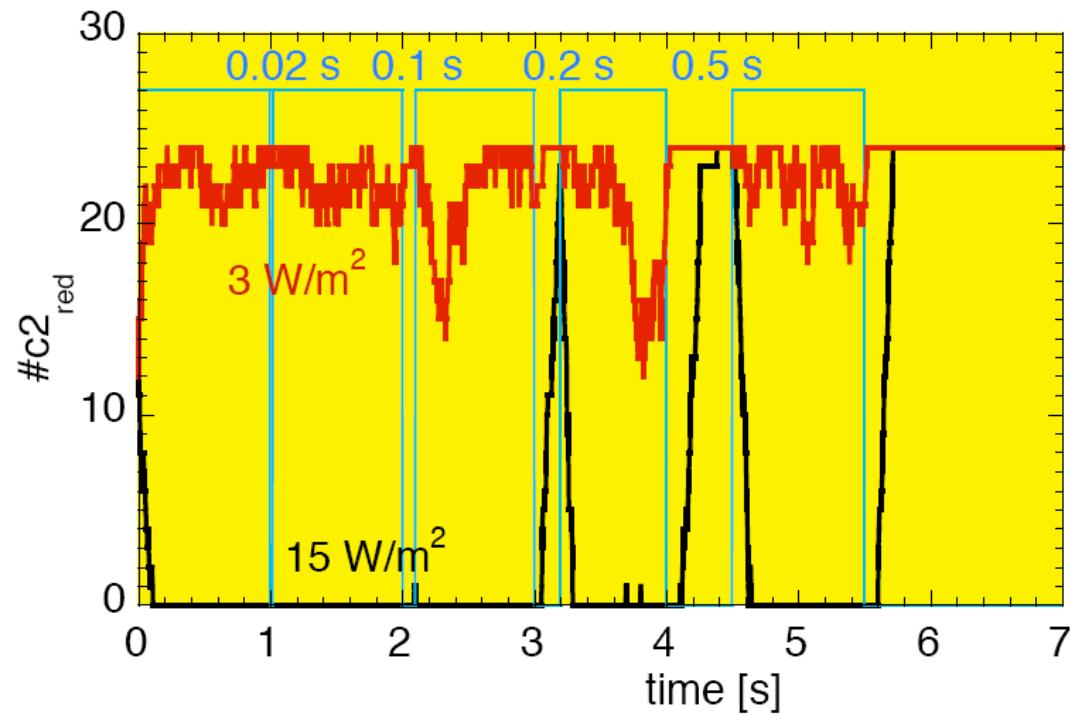
total number of produced ATP



low light intensity: any interruption stops ATP production

high light intensity: interruptions are buffered up to 0.3 s duration

c_2 pool acts as buffer



At high light intensity, c_2 pool is mainly oxidized.

If light is turned off, bc1 can continue to work (load c_2 s, pump protons, let ATPase produce ATP) until c_2 pool is fully reduced.

What if parameters are/were unknown ?

Bridging the Gap: Linking Molecular Simulations and Systemic Descriptions of Cellular Compartments

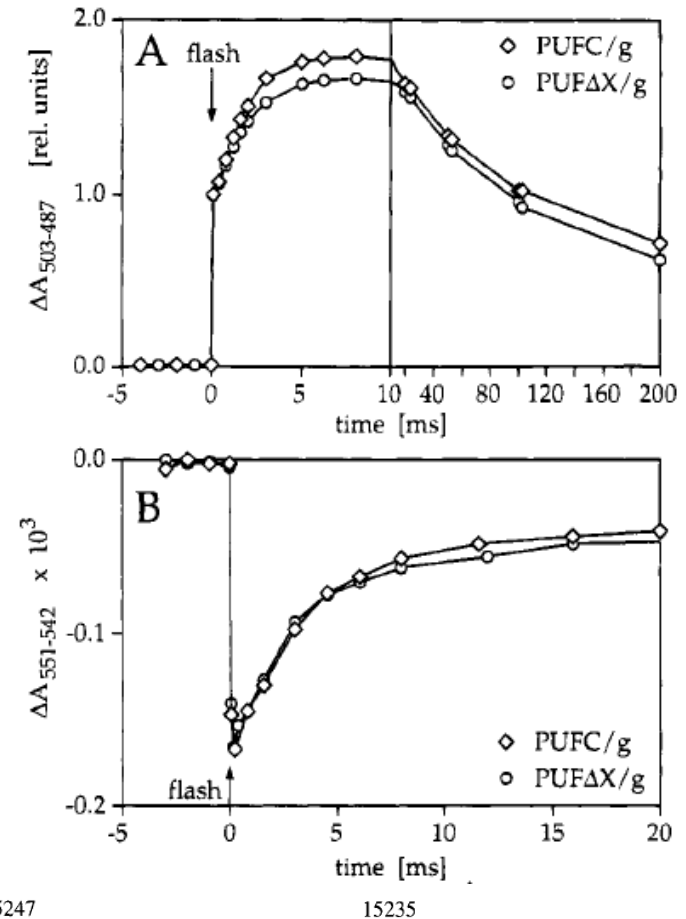
Tihamér Geyer*, Xavier Mol, Sarah Blaß, Volkhard Helms

Center for Bioinformatics, Saarland University, Saarbrücken, Germany

PLoS ONE (2010)

choose 25 out of 45 system parameters
for optimization.

take 7 different non-equilibrium time-resolved
experiments from Dieter Oesterhelt lab
(MPI Martinsried).



Biochemistry 1995, 34, 15235–15247

15235

Role of PufX Protein in Photosynthetic Growth of *Rhodobacter sphaeroides*.

1. PufX Is Required for Efficient Light-Driven Electron Transfer and Photophosphorylation under Anaerobic Conditions[†]

Wolfgang P. Barz,^{‡,§} Francesco Francia,^{||} Giovanni Venturoli,^{||} B. Andrea Melandri,^{||} André Verméglio,[⊥] and Dieter Oesterhelt^{*,‡}

Parameters not optimized

Parameter	Value	Description
$bc_1::k_{on}(H^+_{out})$	$10^{10} \text{ nm}^3 \text{ s}^{-1}$	rate for proton uptake from the cytoplasm by bc_1
$bc_1::k_{tr}(e:Q_0 \Rightarrow FeS)$	$2.3 * 10^3 \text{ s}^{-1}$	rate for electron transfer from Q_0 to FeS
$bc_1::k_{tr}(e:c_1 \Rightarrow c_2)$	10^5 s^{-1}	electron transfer rate from c_1 to bound cytochrome c_2
$bc_1::k_{tr}(e:Q_0 \Rightarrow b_L)$	10^4 s^{-1}	electron transfer from Q_0 to b_L heme
$bc_1::k_{tr}(e:b_L \Rightarrow b_H)$	10^4 s^{-1}	electron transfer from b_L to b_H heme
$\Delta\Phi::V$	$2.65 * 10^4 \text{ nm}^3$	inner volume of the vesicle
$\Delta\Phi::A$	$5.28 * 10^3 \text{ nm}^2$	membrane area (Q pool „volume“)
$\Delta\Phi::C_{H_{in}}$	1.0 e	effective charge of a free proton in the vesicle
$\Delta\Phi::C_{H_{in}}$	1.0 e	effective charge of a proton on the titratable groups
$\Delta\Phi::C_{prot}$	-1.0 e	effective charge of an e^- translocated through an RC
$\Delta\Phi::C_{red}$	-0.5 e	effective charge of a reduced cytochrome c_2
$\Delta\Phi::C_{ox}$	0.5 e	effective charge of an oxidized cytochrome c_2
$PR::N_p$	80	number of titratable groups in the vesicle
$PR::pK$	5.0	pK of the titratable groups
N_{core}	10	number of dimeric core complexes (2 RC + 1 LHC)
N_{bc1}	10	number of cytochrome bc_1 complexes
N_{ATPase}	1	number of ATPases
N_{c2}	20	total number of cytochrome c_2
N_Q	200	total number of quinones

Table S1: Model Parameters Not Included in the Optimization Process

Parameter optimization through evolutionary algorithm

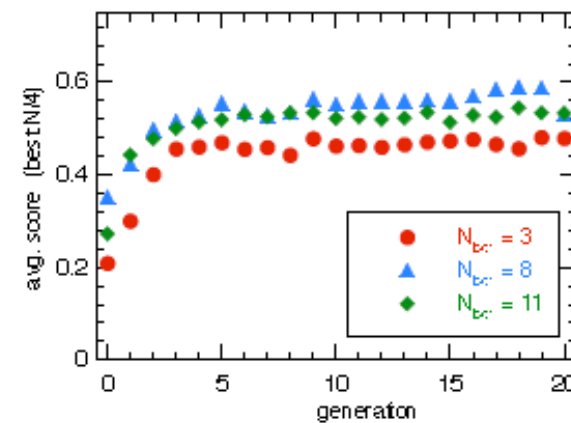
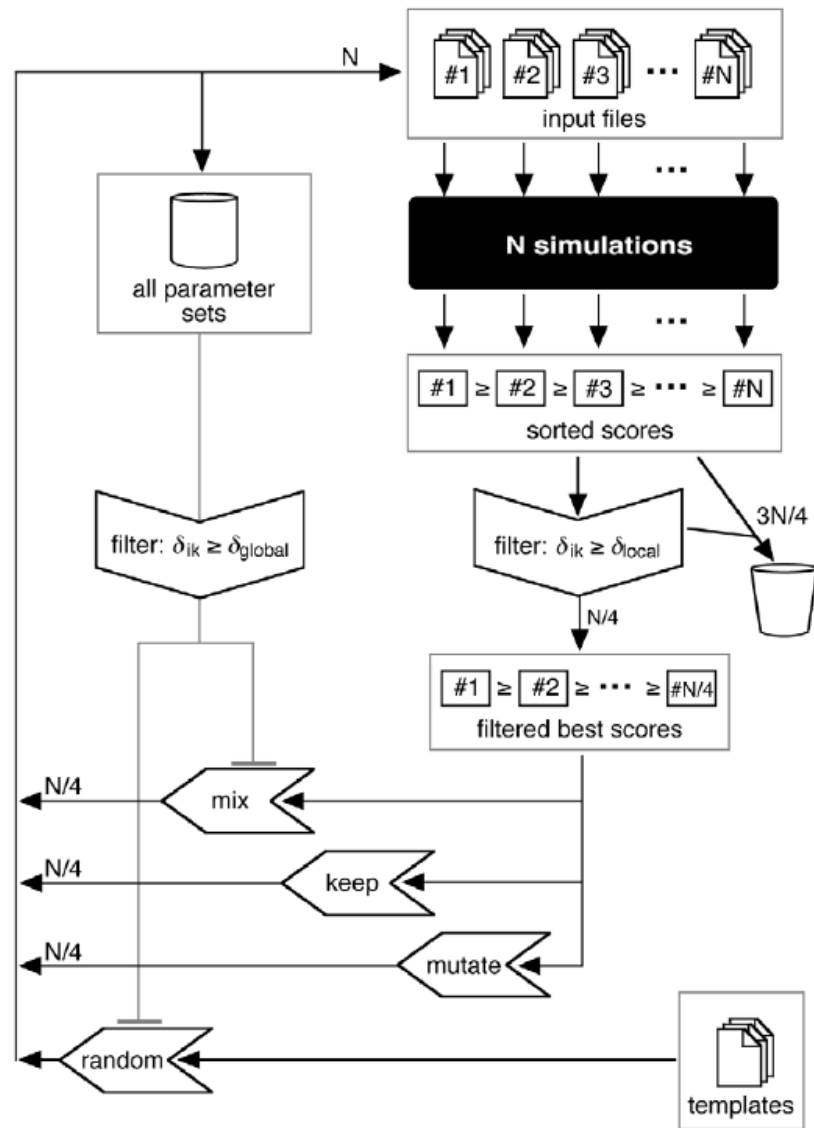


Figure S1: Determining the Number of bc1 Complexes: Evolution of the Master Score

25 optimization parameters

Analyze 1000 best
parameter sets among
32.800 simulations:

$$\langle P \rangle = \exp[\langle \log P \rangle]$$

$$\sigma^2 = \langle (\log P - \langle \log P \rangle)^2 \rangle$$

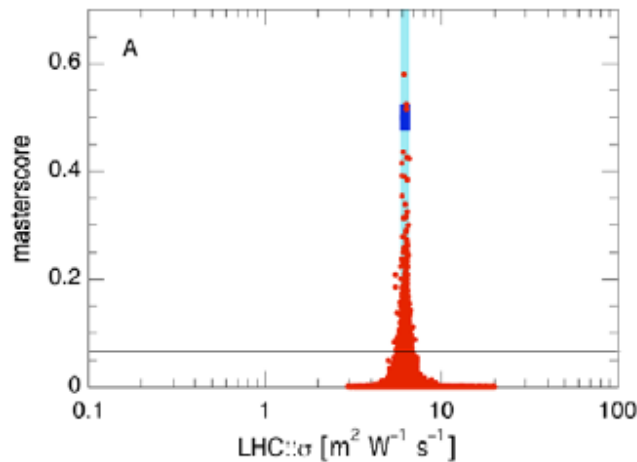
$$P_{\min} = \exp[\langle \log P \rangle - \sigma]$$

$$P_{\max} = \exp[\langle \log P \rangle + \sigma]$$

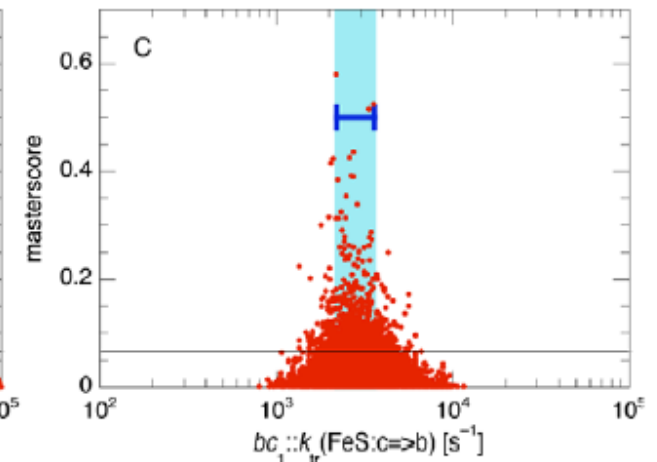
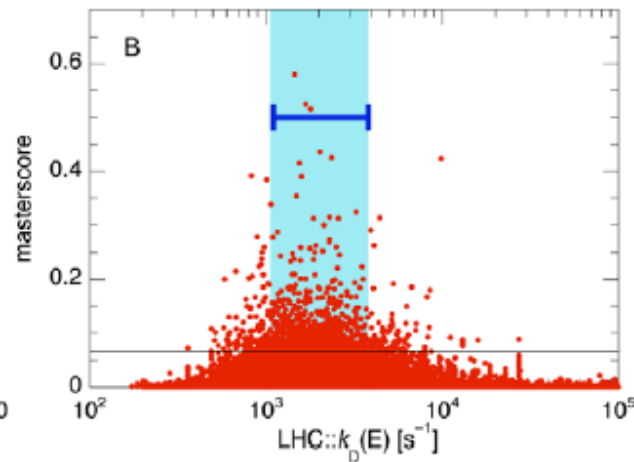
parameter	units	$\langle P \rangle$	$P_{\min} \dots P_{\max}$	P_{\min}/P_{\max}
LHC:: σ	$\text{m}^2 \text{W}^{-1} \text{s}^{-1}$	6.22	6.02...6.42	0.94
LHC:: N_0	1	1.31	0.81 ... 2.13	0.38
LHC:: $k_D(E)$	s^{-1}	$1.9 \cdot 10^3$	$(1.1 \dots 3.8) \cdot 10^3$	0.29
RC:: $k_{on}(E)$	s^{-1}	$24 \cdot 10^6$	$(1.2 \dots 4.5) \cdot 10^6$	0.27
RC:: $k_{on}(H^+)$	$\text{nm}^3 \text{s}^{-1}$	$14 \cdot 10^8$	$(1.3 \dots 1.6) \cdot 10^8$	0.81
RC:: $k_{on}(Q)$	$\text{nm}^2 \text{s}^{-1}$	$6.0 \cdot 10^4$	$(4.4 \dots 8.1) \cdot 10^4$	0.54
RC:: $k_{off}(QH2)$	s^{-1}	87	70...108	0.65
RC:: $k_{on}(c2red)$	$\text{nm}^3 \text{s}^{-1}$	$9.2 \cdot 10^5$	$(7.3 \dots 11.5) \cdot 10^5$	0.63
RC:: $k_{off}(c2ox)$	s^{-1}	$2.2 \cdot 10^3$	$(1.6 \dots 3.0) \cdot 10^3$	0.53
bc1:: $k_{on}(QH2@Q_0)$	$\text{nm}^2 \text{s}^{-1}$	$1.2 \cdot 10^4$	$(0.79 \dots 1.7) \cdot 10^4$	0.46
bc1:: $k_{off}(Q@Q_0)$	s^{-1}	28.3	26.3...30.4	0.86
bc1:: $k_{tr}(Q:Q_0 \rightarrow Q_i)$	s^{-1}	$4.9 \cdot 10^3$	$(3.6 \dots 6.7) \cdot 10^3$	0.54
bc1:: $k_{on}(Q@Q_i)$	$\text{nm}^2 \text{s}^{-1}$	$6.7 \cdot 10^5$	$(4.5 \dots 10) \cdot 10^5$	0.45
bc1:: $k_{off}(QH2@Q_i)$	s^{-1}	86	68...110	0.62
bc1:: $k_{tr}(QH2:Q_i \rightarrow Q_0)$	s^{-1}	$3.8 \cdot 10^3$	$(2.6 \dots 5.5) \cdot 10^3$	0.47
bc1:: $k_{on}(c2ox)$	$\text{nm}^3 \text{s}^{-1}$	$94 \cdot 10^6$	$(6.3 \dots 14) \cdot 10^6$	0.47
bc1:: $k_{off}(c2red)$	s^{-1}	$6.0 \cdot 10^3$	$(3.3 \dots 11) \cdot 10^3$	0.30
bc1:: $k_{off}(H+@Q_0)$	s^{-1}	$24 \cdot 10^4$	$(1.3 \dots 4.3) \cdot 10^4$	0.30
bc1:: $k_{tr}(Fe5:b \rightarrow c)$	s^{-1}	$3.9 \cdot 10^3$	$(3.1 \dots 5.1) \cdot 10^3$	0.61
bc1:: $k_{tr}(Fe5:c \rightarrow b)$	s^{-1}	$2.8 \cdot 10^3$	$(2.2 \dots 3.6) \cdot 10^3$	0.61
bc1:: $k_{tr}(e:b_H \rightarrow Q_i)$	s^{-1}	$7.7 \cdot 10^3$	$(5.0 \dots 12) \cdot 10^3$	0.42
bc1:: Φ_0	mV	102	83...114	0.73
$\Delta\Phi::U_0$	mV/e	10.3	9.5...11	0.85
$\Delta\Phi::\Delta\Phi_0$	mV/pH	10	7.6...13.7	0.55
PR::pK	1	4.84	3.9...5.9	0.66

Sensitivity of master score

Decay rate of excitons
in LHC



Absorption cross section
light harvesting complex



Kinetic rate for hinge
motion of FeS domain in
bc1 complex

Some parameters are very sensitive, others not.

Three best-scored parameter sets

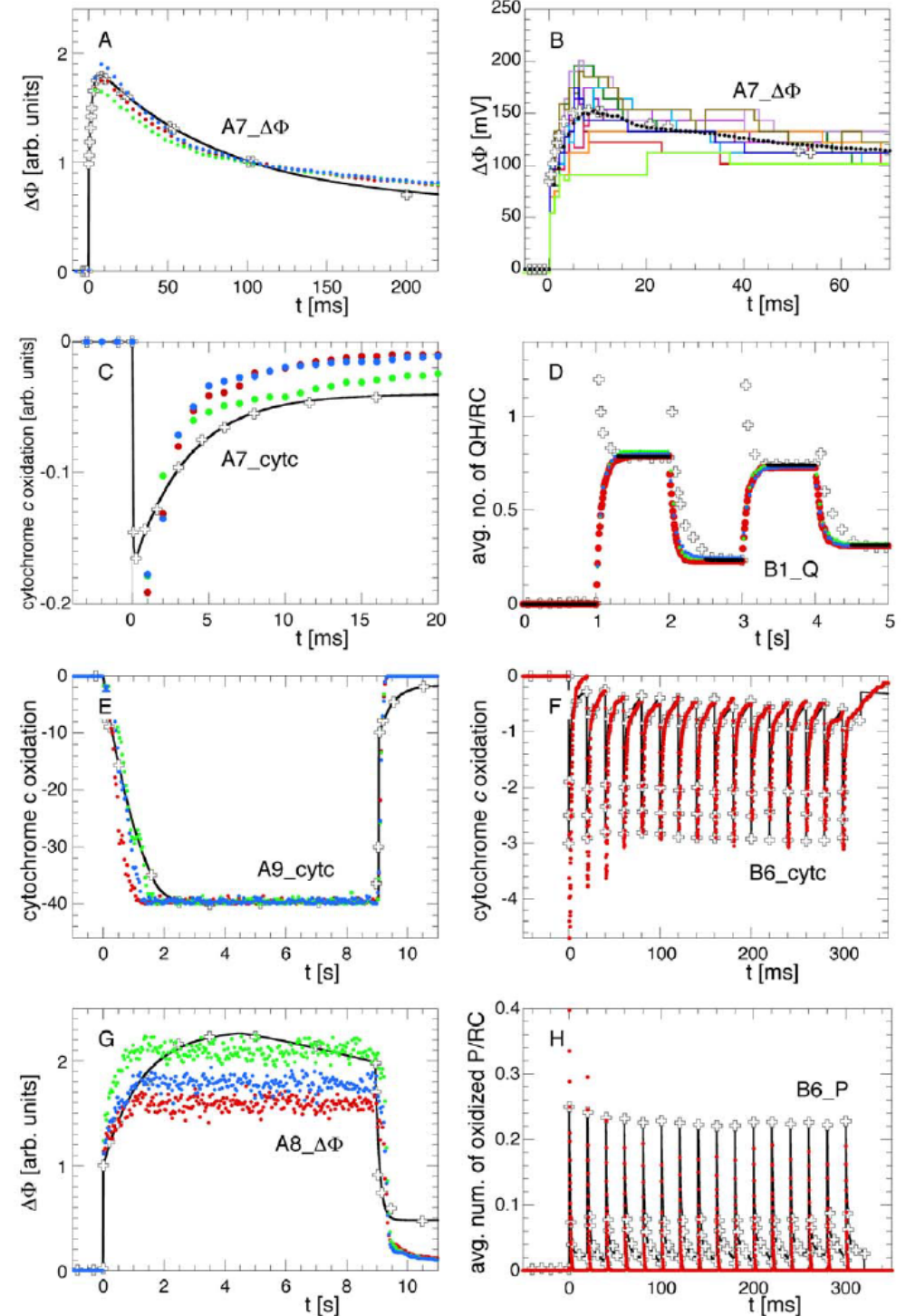
Score of individual parameter set i
for matching one experiment:

$$s_i = \frac{C_i}{\sum (x(t_i) - f(t_i))^2}$$

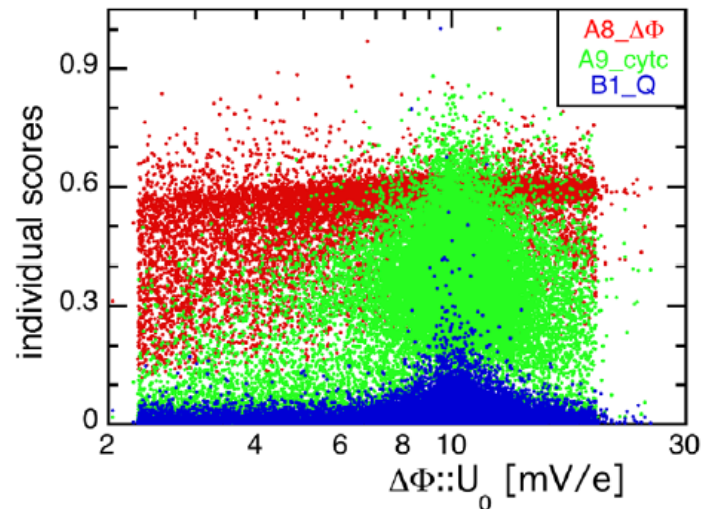
$x(t_i)$: simulation result

$f(t_i)$: smooth fit of exp. data

Master score for one
parameter set: defined as
product of the individual
scores s_i



Different experiments yield different sensitivity



“importance score”:
Sum of the sensitivities
 P_{min}/P_{max} of all relevant
parameters

Table 2. Importance scores and correlation coefficients between the master score and the respective individual scores of the experimental scenarios denoting the relative importance of each of the experiments for the parameter value optimization.

experiment	A7 cytc	A7 $\Delta\Phi$	A8 $\Delta\Phi$	A9 cytc	B1 Q	B6 P	B6 cytc	BC1
importance score	4.4	7.7	5.8	9.7	3.8	5.2	8.9	5.5
correlation	0.09	0.44	0.22	0.38	0.83	0.17	0.31	0.41

The importance scores are determined as the sums of the sensitivities of all relevant parameters against the individual scores (see table S2 for all the individual values). The correlation coefficients are obtained from a linear fit of the master score against the respective individual score.

Analysis could suggest new
experiments that would be
most informative!

Summary

Only 1/3 of the kinetic parameters previously known.

Stochastic parameter optimization converges robustly into the same parameter basin as known from experiment.

Two large-scale runs (15 + 17 parameters) yielded practically the same results.

If implemented as grid search, less than 2 points per dimension.

It appears enough to know 1/3 – 1/2 of kinetic rates about a system to be able to describe it quantitatively (IF connectivities are known).

Review – algorithms / methods etc in Bioinfo III

“There is no such thing as a free lunch”.

Alvin Hansen, economist (1953)

There exist several “No Free Lunch Theorems” for optimization problems.

E.g. Wolpert & Macready (1997) showed:

For any search/optimization algorithm, any elevated performance over one class of problems is exactly paid for in performance over another class.

Review – simulation / analysis methods

	Used where	Pro	Con
Enrichment methods	Annotate gene function, histone peaks, motifs	Proper statistical analysis	Not causal, mechanistic reasons remain unclear
Graph algorithms	Modules in PPI networks, PP complexes, MCDS algo for key genes in GRNs, Cut-sets in metabolic networks	<ul style="list-style-type: none">- graph layout provides intuitive view of network topology,- ILPs give optimal solutions,- heuristic algorithms can be fast	<ul style="list-style-type: none">- ILPs very time-consuming,- heuristic solutions may be not accurate,- graph algorithms suffer from noisy data

Review – simulation / analysis methods

	Used where	Pro	Con
Pearson correlation	Gene co-expression, DNA co-methylation	Quantitative measure	Suffers from outliers (V21); correlations are not causal
Rank-based correlation	Gene co-expression	Avoids outlier problems	Sensitive to small variations, large variations may be condensed into small rank differences
Bayesian network	Anywhere (here: PPIs)	Integrates arbitrary data; automatic weighting of likelihoods	Not causal (but this can be included)
Boolean network	GRNs	Finite state space, understand system completely, causal	Values restricted to boolean levels (but can be generalized)

Review – simulation / analysis methods

	Used where	Pro	Con
FBA	Metabolic networks	Gives one optimal solution	None (?)
EFMs / EPs	Metabolic networks	Full insight into metabolic capabilities of system	Already medium-sized systems have 10.000s + EFMs
ODE	Metabolic systems, Signaling systems	Quantitative, time-dependent models, simple systems can be solved analytically, simple numerical implementation	Needs many parameters, not suitable for small particle numbers
Stochastic simulations	Metabolic systems	Capture stochastic effects of few particles,	Not deterministic (different solution each time); costly